An Alternate Pattern for Globoside Oligosaccharide Expression in *Haemophilus influenzae* Lipopolysaccharide: Structural Diversity in Nontypeable Strain 1124

Håkan H. Yildirim,[‡] Jianjun Li,[§] James C. Richards,[§] Derek W. Hood,[||] E. Richard Moxon,[||] and Elke K. H. Schweda*,[‡]

Clinical Research Centre, Karolinska Institutet and University College of South Stockholm, NOVUM, S-141 86 Huddinge, Sweden, Institute for Biological Sciences, National Research Council of Canada, Ottawa, Ontario, Canada K1A OR6, and Molecular Infectious Diseases Group and Department of Paediatrics, Weatherall Institute of Molecular Medicine, John Radcliffe Hospital, Oxford, U.K.

Received December 1, 2004; Revised Manuscript Received January 25, 2005

ABSTRACT: Common structural motifs of *Haemophilus influenzae* lipopolysaccharide (LPS) are globotetraose [β-D-Gal*p*NAc-(1→3)-α-D-Gal*p*-(1→4)-β-D-Gal*p*-(1→4)-β-D-Glc*p*] and its truncated versions globoside [α-D-Gal*p*-(1→4)-β-D-Gal*p*-(1→4)-β-D-Glc*p*] and lactose [β-D-Gal*p*-(1→4)-β-D-Glc*p*] linked to the terminal heptose (HepIII) of the triheptosyl inner-core moiety L-α-D-Hep*p*-(1→2)-[*P*EA→6]-L-α-D-Hep*p*-(1→3)-L-α-D-Hep*p*-(1→5)-[*PP*EA→4]-α-Kdo-(2→6)-lipid A. We report here structural studies of LPS from nontypeable *H. influenzae* strain 1124 expressing these motifs linked to both the proximal heptose (HepI) and HepIII at the same time. This novel finding was obtained by structural studies of LPS using NMR techniques and electrospray ionization mass spectrometry (ESI-MS) on O-deacylated LPS and core oligosaccharide material (OS) as well as ESI-MS^n on permethylated dephosphorylated OS. The use of defined mutants allowed us to confirm structures unambiguously and understand better the biosynthesis of each of the globotetraose units. We found that *lgtC* is involved in the expression of α-D-Gal*p*-(1→4)-β-D-Gal*p* in both extensions, whereas *lic2A* directs only the expression of β-D-Gal*p*-(1→4)-β-D-Glc*p* when linked to HepIII. The LPS of NTHi strain 1124 contained sialylated glycoforms that were identified by CE-ESI-MS/MS. A common sialylated structure in *H. influenzae* LPS is sialyllactose linked to HepIII. This structure exists in strain 1124. However, results for the *lpsA* mutant indicate that sialyllactose extends from HepI as well, a molecular environment for sialyllactose in *H. influenzae* that has not been reported previously. In addition, the LPS was found to carry phosphorylcholine, O-linked glycine, and a third *P*EA group which was linked to O3 of HepIII.

Haemophilus influenzae is an important cause of human disease worldwide and exists in encapsulated (type a−f) and unencapsulated (nontypeable) forms. Type b capsular strains are associated with invasive bacteraemic diseases, including meningitis, epiglottis, cellulitits, and pneumonia, while acapsular or nontypeable strains of *H. influenzae* (NTHi)[1] are primary pathogens in otitis media and both acute and chronic lower respiratory tract infections (*1*). The potential of *H. influenzae* to cause disease depends on its surface-expressed carbohydrate antigens, capsular polysaccharide (*2*), and lipopolysaccharide (LPS) (*3*).

LPS is an essential and characteristic surface component of *H. influenzae*. This bacterium has been found to express short-chain LPS, lacking O-specific polysaccharide chains and often termed lipooligosaccharide (LOS). Extensive structural studies of LPS from *H. influenzae* by us and others have led to the identification of a conserved glucose-substituted triheptosyl inner-core moiety L-α-D-Hep*p*-(1→2)-[*P*EA→6]-L-α-D-Hep*p*-(1→3)-[β-D-Glc*p*-(1−4)]-L-α-D-Hep*p* linked to lipid A via 3-deoxy-D-*manno*-oct-2-ulosonic acid (Kdo) 4-phosphate. This inner-core unit provides the template for attachment of oligosaccharide and noncarbohydrate substituents (*4*−*23*). LPS of *H. influenzae* can mimic host glycolipids and has a propensity for reversible switching of expression of saccharide and noncarbohydrate epitopes (phase variation), leading to considerable intrastrain variation in structure. Phase variation is thought to provide an adaptive mechanism which is advantageous for survival of bacteria confronted by the differing microenvironments and immune responses of the host (*24*). Terminal structures mimicking the globoside series of mammalian glycolipids have been identified. These include galabiose [α-D-Gal*p*-(1→4)-β-D-Gal*p*-(1→], lactose [β-D-Gal*p*-(1→4)-β-D-Glc*p*-(1→], sialyllactose [α-Neu5Ac-(2→3)-β-D-Gal*p*-(1→4)-β-D-Glc*p*-(1→], and globotetraose [β-D-Gal*p*NAc-(1→3)-α-D-Gal*p*-

* To whom correspondence should be addressed: University College of South Stockholm, Clinical Research Center, NOVUM, S-141 86 Huddinge, Sweden. Telephone: + 46 8 585 838 23. Fax: + 46 8 585 838 20. E-mail: elke.schweda@kfc.ki.se.

‡ Karolinska Institutet and University College of South Stockholm.

§ National Research Council of Canada.

|| John Radcliffe Hospital.

[1] Abbreviations: CE, capillary electrophoresis; Kdo, 3-deoxy-D-*manno*-oct-2-ulosonic acid; *An*Kdo-ol, reduced anhydro-Kdo; Hep, heptose; L,D-Hep, L-*glycero*-D-*manno*-heptose; Hex, hexose; LPS-OH, O-deacylated lipopolysaccharide; lipid A-OH, O-deacylated lipid A; LPS, lipopolysaccharide; MS^n, multiple-step tandem mass spectrometry; Neu5Ac, *N*-acetylneuraminic acid; NTHi, nontypeable *H. influenzae*; OS, oligosaccharide; *P*Cho, phosphocholine; *P*EA, phosphoethanolamine; *PP*EA, pyrophosphoethanolamine; Ac, acetate; Gly, glycine.

10.1021/bi047480h CCC: $30.25
Published on Web 03/08/2005

(1→4)-β-D-Gal*p*-(1→4)-β-D-Glc*p*-(1→]. The genes involved in LPS biosynthesis have been investigated extensively in type b strain Eagan and in genome reference strain Rd (*25*, *26*). The genes required for oligosaccharide initiation from each of the three heptose residues in the inner core have been identified as *lgtF*, *lic2C*, and *lpsA* (*27*). A genetic mechanism, polymerase slippage in runs of tetranucleotide repeats, directs LPS phase variation in five characterized chromosomal loci [*lic1*, *lic2*, *lic3*, *lgtC*, and *lex2* (*28*−*30*)]. The *lex2* locus has been shown to encode a glucosyltransferase adding a second β-D-Glc*p* to the glucose (GlcI) linked to the proximal heptose (HepI) in the inner core and is important for further oligosaccharide extension (*31*). It has been demonstrated that expression of *P*Cho substituents in *H. influenzae* LPS is subject to phase variation mediated by the *lic1* locus (*32*). Genes comprising the *lic2* locus have been shown to be required for chain extension from the middle heptose (HepII) (*27*), and together with *lgtC*, the *lic2A* gene is responsible for the phase variable expression of the galabiose component of the globoside oligosaccharide [α-D-Gal*p*-(1→4)-β-D-Gal*p*-(1→4)-β-D-Glc*p*-(1→]. The globoside epitope has been identified in some strains as a trisaccharide extension attached directly from the distal heptose (HepIII) (*9*, *18*, *19*, *21*, *33*) or as the terminal moiety of a tetrasaccharide extension from HepI (*20*, *22*) and/or the central heptose (HepII) (*7*, *21*, *22*). The *lic3* locus encodes an α-2,3-sialyltransferase that is responsible for addition of sialic acid (*N*-acetylneuraminic acid or Neu5Ac) to terminal lactose elongating from HepIII (*34*).

Our previous studies have focused on the extent of conservation and variability of LPS expression in a representative set of clinical isolates of NTHi obtained from otitis media patients (*13*, *16*−*20*) and relating this to the role of the molecule in commensal and virulence behavior. Recently, we demonstrated that terminal sialic acid-containing oligosaccharide epitopes are essential virulence determinants in experimental otitis media (*35*).

In this paper, we report on the structures and expression of LPS glycoforms of NTHi strain 1124. The wild-type strain was found to express a complex mixture of LPS glycoforms. To determine structures unambiguously, we made use of genetically defined isogenic mutant strains, including *lpsA*, *lic2A*, and *lgtC*, to truncate independent oligosaccharide extensions. This combination of genetics and detailed structural analysis enabled us to demonstrate that NTHi 1124 expresses novel LPS glycoforms containing globoside epitopes and their biosynthetic intermediates extending simultaneously from both the proximal and distal heptose residues. Mono- and disialyl lactose units substituting one heptose residue, the other heptose residue, or both were characterized which likely contribute to the resistance of the strain to killing by normal human serum (*33*).

EXPERIMENTAL PROCEDURES

Construction of Mutant Strains. NTHi strain 1124 was obtained from the Finnish Otitis Media Study Group and is an isolate obtained from the middle ear (*36*). The parent strain will be termed 1124wt for clarity. Mutant strains were constructed following transformation (*37*) of isolate 1124 using plasmid and chromosomal DNA constructs containing the relevant gene interrupted by an antibiotic resistance cassette, as described previously (*25*). Strains 1124*lpsA* and 1124*lgtC* were made by transformation with plasmids $p11_2$ and pH2, respectively, described previously (*25*), and strain 1124*lic2A* was constructed by transformation with chromosomal DNA derived from a *lic2A* mutant of strain RM118 (*26*). Each mutant strain was confirmed after growth on BHI-kanamycin (10 μg/mL) by PCR and Southern analyses.

Bacterial Growth and LPS Preparation. Bacteria were grown in brain−heart infusion broth supplemented with haemin (10 μg/mL), NAD (2 μg/mL), and, in one experiment, Neu5Ac (10 μg/mL; NTHi 1124wt). LPS was extracted from lyophilized bacteria using phenol, chloroform, and light petroleum as described previously but with the modification that the LPS was precipitated with 6 volumes of diethyl ether and acetone (1:5, by volume) (*38*). LPS was purified by ultracentrifugation (82000*g* for 12 h at 4 °C).

Analysis of Lipopolysaccharide by Electrophoresis. Isolated LPS was analyzed by tricine−sodium dodecyl sulfate−polyacrylamide gel electrophoresis (T−SDS−PAGE) and staining with silver (Quicksilver, Amersham Pharmacia) (*25*).

Chromatography. Gel filtration chromatography was performed using a Bio-Gel P4 column (2.5 cm × 80 cm) with pyridinium acetate (0.1 M, pH 5.3) as an eluent and a differential refractometer as a detector.

Preparation of Oligosaccharides. (a) O-Deacylation of LPS with Hydrazine. O-Deacylation of LPS was achieved as previously described (*39*). Briefly, LPS (1 mg) was mixed with anhydrous hydrazine (0.1 mL) and stirred at 37 °C for 1 h. The reaction mixture was cooled, and cold acetone (1 mL) was added to destroy excess hydrazine. The precipitated O-deacylated LPS (LPS-OH) was centrifuged (48200*g* for 20 min), and the pellet was washed twice with cold acetone and once with diethyl ether and then dissolved in water followed by lyophilization.

(b) Mild Acid Hydrolysis of LPS. Core oligosaccharide fractions were obtained following mild acid hydrolysis of LPS (30 mg of 1124wt, 30 mg of 1124*lpsA*, 40 mg of 1124*lic2A*, and 40 mg of 1124*lgtC*, in 1% acetic acid at pH 3.1 and 100 °C for 2 h). The reducing agent, the borane−*N*-methylmorpholine complex (3−4 mg), was included in the hydrolysis mixture. The insoluble lipid A (10 mg for 1124wt, 10 mg for 1124*lpsA*, 17 mg for 1124*lic2A*, and 17 mg for 1124*lgtC*) was separated from the hydrolysis mixtures by centrifugation. Following purification on the Biogel P4 column, oligosaccharide fractions (8.7 mg of OS1124wt, 5.6 mg of OS1124*lpsA*, 15 mg of OS1124*lic2A*, and 13.5 mg of OS1124*lgtC*) were obtained.

(c) Dephosphorylation. One milligram of the oligosaccharide samples was incubated with 48% hydrogen fluoride (HF) (0.1 mL) for 48 h at 4 °C. Then, the samples were placed into an ice bath, and HF was evaporated under a stream of nitrogen gas. The samples were dissolved in water and lyophilized.

Mass Spectrometry. GLC−MS was carried out with a Hewlett-Packard 6890 chromatograph connected to a Micromass quadrupole mass spectrometer using a DB-5 fused silica capillary column [25 m × 0.25 mm (0.25 μm inside diameter)] and a temperature gradient from 130 (1 min) to 250 °C at 3 °C/min.

Electrospray ionization mass spectrometry (ESI-MS) on LPS-OH and OS samples was carried out with a VG Quattro triple-quadrupole mass spectrometer (Micromass, Manches-

ter, U.K.) in the negative ion mode. The samples were dissolved in a mixture of water and acetonitrile (1:1, v/v). Sample solutions were injected via a syringe pump into a running solvent of water and acetonitrile (1:1, v/v) at a flow rate of 10 μL/min. Multiple-step tandem ESI-MS (ESI-MS^n) experiments on permethylated OS samples were performed in the positive ion mode on a Finnigan LCQ ion-trap mass spectrometer (Finnigan-MAT, San Jose, CA). Samples were dissolved in 1 mM sodium acetate in methanol and water (7:1, v/v) at a flow rate of 10 μL/min. CE-ESI-MS^n was carried out with a Crystal model 310 CE instrument (ATI Unicam, Boston, MA) coupled to an API 3000 mass spectrometer (Perkin-Elmer/Sciex, Concord, ON) via a MicroIonspray interface as described previously (*16*)

Analytical Methods. Sugars were identified by GLC−MS as their alditol acetates or (+)-2-butyl-acetylated glycosides as previously described (*40*, *41*). Methylation was performed with methyl iodide in dimethyl sulfoxide in the presence of lithium methylsulfinylmethanide (*42*). The methylated compounds were recovered using a SepPak C18 cartridge and subjected to sugar analysis or ESI-MS^n. The relative proportions of the various alditol acetates and partially methylated alditol acetates obtained in sugar and methylation analyses, discussed below, correspond to the detector response of GLC−MS. Fatty acids were identified as previously described (*43*).

NMR Spectroscopy. NMR spectra were recorded for OS samples in deuterium oxide (D_2O) at 22, 25, 22, and 30 °C for 1124*lpsA*, 1124*lic2A*, 1124*lgtC*, and 1124wt, respectively. The NMR experiments were carried out at different temperatures to prevent overlap of the HDO peak with anomeric proton signals in the various samples. Spectra were acquired on a JEOL 500 MHz spectrometer using standard pulse sequences. Chemical shifts were reported in parts per million, and referenced to external sodium 3-trimethylsilylpropanoate-d_4 (δ 0.00, ^{1}H), external acetone (δ 30.1, ^{13}C), and external trimethyl phosphate (δ 2.00, ^{31}P). ^{1}H−^{1}H gradient-selected correlated spectroscopy (gCOSY), gradient-selected total correlation spectroscopy (gTOCSY) with a mixing time of 180 ms, gradient-selected heteronuclear single-quantum coherence (gHSQC), gradient-selected heteronuclear multiple-quantum coherence (gHMQC), and gradient-selected heteronuclear multiple-bond correlation (gHMBC) experiments were performed according to standard pulse sequences. For interresidue correlation, two-dimensional gradient-selected nuclear Overhauser effect spectroscopy (gNOESY) experiments with a mixing time of 250 ms were used.

RESULTS

NTHi Wild-Type Strain 1124 and Isogenic Mutants 1124lpsA, 1124lic2A, and 1124lgC. H. influenzae nontypeable strain 1124 (1124wt) is a clinical isolate from otitis media obtained by the Finnish Otitis Media Study Group. Preliminary structural studies indicated that this strain produces heterogeneous mixtures of LPS glycoforms (see below). To facilitate structural analysis, we constructed defined mutants in known biosynthetic genes that would limit some oligosaccharide extensions, thus simplifying analyses of the remaining glycoforms in their LPS. It was recently shown that the *lpsA* gene is involved in initiating chain elongation from the distal Hep (HepIII) of the inner-core region (*26*). Therefore, we predicted that the LPS of a *lpsA* mutant of NTHi strain 1124 would not exhibit chain elongation from HepIII in its LPS, but would be otherwise structurally identical to the LPS of the parent strain. The *lic2A* and *lgtC* genes have been shown to encode glycosyltransferases involved in sequential addition of β-1,4-linked Gal*p* (*lic2A*) and α-1,4-Gal*p* (*lgtC*) to β-Glc*p* residues (*26*). The LPS from *lgtC* and *lic2A* mutants of 1124 would therefore be predicted to include glycoforms sequentially truncated in globoside extensions [i.e., α-D-Gal*p*-(1→4)-β-D-Gal*p*-(1→4)-β-D-Glc*p*-(1→].

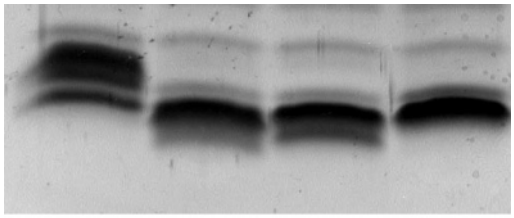

FIGURE 1: T−SDS−PAGE patterns of LPS from NTHi strains 1124wt, 1124*lic2A*, and 1124*lgtC*.

Table 1: Sugar Analysis Data for LPS-OH and OS Samples Derived from *H. influenzae* Strains 1124wt, 1124*lpsA*, 1124*lic2A*, and 1124*lgtC*

	relative detector response (%)							
	1124wt		1124*lpsA*		1124*lic2A*		1124*lgtC*	
sugar residue[a]	OS	LPS-OH	OS	LPS-OH	OS	LPS-OH	OS	LPS-OH
Glc	17	27	3	18	21	28	27	22
Gal	55	44	84	40	47	42	39	31
Hep	23	12	12	18	31	13	34	28
GlcN		16		19		16		19
GalN	5	1	1	5	1	1		

[a] Sugars were identified by GLC−MS as their alditol acetate.

Isolation and Characterization of LPS from NTHi Wild-Type Strain 1124 and Its Mutants. All strains were grown in liquid culture, and LPS was isolated by the phenol/chloroform/light petroleum extraction method (*38*). Tricine−sodium dodecyl sulfate−polyacrylamide gel electrophoresis (T−SDS−PAGE) analysis showed that 1124wt LPS was a heterogeneous mixture comprised of several bands, whereas mutant strains 1124*lpsA*, 1124*lic2A*, and 1124*lgtC* produced truncated glycoforms (Figure 1). O-Deacylation of LPS material by treatment with anhydrous hydrazine under mild conditions afforded water-soluble material (LPS-OH). Compositional analysis of the LPS-OH samples for 1124wt, 1124*lpsA*, 1124*lic2A*, and 1124*lgtC* identified D-glucose (Glc), D-galactose (Gal), 2-amino-2-deoxygalactose (GalN), 2-amino-2-deoxyglucose (GlcN), and L-*glycero*-D-*manno*-heptose (Hep) as the constituent sugars by GLC−MS analysis of the derived alditol acetate and 2-butyl glycoside derivatives on oligosaccharide material (Table 1). Significant amounts of Gal were detected in wild-type and mutant strains, indicating a predominance of this hexose in the oligosaccharide chains extending from the triheptosyl region. In earlier investigations, it was found that the LPS of 1124wt contained ester-linked glycine and Neu5Ac as shown by HPAEC-PAD, following treatment of samples with 0.1 M NaOH and neuraminidase, respectively (*44*, *45*).

Table 2: Negative Ion ESI-MS Data and Proposed Compositions for O-Deacylated LPS (LPS-OH) and Oligosaccharide (OS) Samples of *H. influenzae* NTHi Strains 1124wt, 1124*lpsA*, 1124*lic2A*, and 1124*lgtC*[a]

	observed ion (*m*/*z*)			molecular mass (Da)		relative abundance (%)				
sample	$(M-4H)^{4-}$	$(M-3H)^{3-}$	$(M-2H)^{2-}$	observed	calculated	wt	*lpsA*	*lic2A*	*lgtC*	proposed composition
LPS-OH	639.6[c]	853.7[c]		2563.2	2565.1		9		6	*P*Cho·Hex_2·Hep_3·*P*EA_2·*P*·Kdo·lipid A-OH
	670.3[c]	894.7[c]		2686.4	2688.2		16		5	*P*Cho·Hex_2·Hep_3·*P*EA_3·*P*·Kdo·lipid A-OH
	680.8	908.3		2727.9	2727.3	4	25	18	5	*P*Cho·Hex_3·Hep_3·*P*EA_2·*P*·Kdo·lipid A-OH
	711.0	949.3		2850.9	2850.3	3	45	27	11	*P*Cho·Hex_3·Hep_3·*P*EA_3·*P*·Kdo·lipid A-OH
	721.3	962.1		2889.3	2889.4	4	4	24	27	*P*Cho·Hex_4·Hep_3·*P*EA_2·*P*·Kdo·lipid A-OH
	752.5	1003.5		3013.8	3012.5	4		25	46	*P*Cho·Hex_4·Hep_3·*P*EA_3·*P*·Kdo·lipid A-OH
	762.1	1016.3		3052.2	3051.5	8		3		*P*Cho·Hex_5·Hep_3·*P*EA_2·*P*·Kdo·lipid A-OH
	772.9	1030.1		3094.5	3093.1	3				*P*Cho·HexNAc·Hex_4·Hep_3·*P*EA_2·*P*·Kdo·lipid A-OH
	792.9	1057.1		3175.0	3174.6	8				*P*Cho·Hex_5·Hep_3·*P*EA_3·*P*·Kdo·lipid A-OH
	803.1	1070.4		3215.3	3213.7	15				*P*Cho·Hex_6·Hep_3·*P*EA_2·*P*·Kdo·lipid A-OH
	812.8	1084.2		3255.4	3255.5	7				*P*Cho·$HexNac_1$·Hex_5·Hep_3·*P*EA_2·*P*·Kdo·lipid A-OH
	833.5	1111.3		3337.5	3336.7	18				*P*Cho·Hex_6·Hep_3·*P*EA_3·*P*·Kdo·lipid A-OH
	843.5	1125.2		3378.3	3378.5	9				*P*Cho·$HexNac_1$·Hex_5·Hep_3·*P*EA_3·*P*·Kdo·lipid A-OH
	853.7	1138.0		3417.9	3417.6	8				*P*Cho·$HexNac_1$·Hex_6·Hep_3·*P*EA_2·*P*·Kdo·lipid A-OH
	884.1	1178.9		3540.1	3540.6	9				*P*Cho·$HexNac_1$·Hex_6·Hep_3·*P*EA_3·*P*·Kdo·lipid A-OH
OS			684.2[c]	1370.4	1372.0		3			*P*Cho·Hex_1·Hep_3·*P*EA_2·*An*Kdo-ol
			712.7[c]	1427.4	1429.0		3			*P*Cho·Gly·Hex_1·Hep_3·*P*EA_2·*An*Kdo-ol
			742.6[b]	1487.2	1486.1			4		*P*Cho·Gly_2·Hex_1·Hep_3·*P*EA_2·*An*Kdo-ol
			765.5[b]	1533.0	1534.1		11	8	3	*P*Cho·Hex_2·Hep_3·*P*EA_2·*An*Kdo-ol
			794.0[b]	1590.0	1591.2		11	4	3	*P*Cho·Gly·Hex_2·Hep_3·*P*EA_2·*An*Kdo-ol
			822.8[b]	1647.6	1648.2			13	3	*P*Cho·Gly_2·Hex_2·Hep_3·*P*EA_2·*An*Kdo-ol
			847.3	1696.6	1696.3	5	39	19	10	*P*Cho·Hex_3·Hep_3·*P*EA_2·*An*Kdo-ol
			875.3	1752.6	1753.3	3	25	13	9	*P*Cho·Gly·Hex_3·Hep_3·*P*EA_2·*An*Kdo-ol
			904.7	1811.4	1810.4			8	13	*P*Cho·Gly_2·Hex_3·Hep_3·*P*EA_2·*An*Kdo-ol
			927.9	1857.8	1858.4	7	5	16	37	*P*Cho·Hex_4·Hep_3·*P*EA_2·*An*Kdo-ol
			956.9	1915.8	1915.5	4	3	14	19	*P*Cho·Gly·Hex_4·Hep_3·*P*EA_2·*An*Kdo-ol
			985.0	1972.0	1972.5				12	*P*Cho·Gly_2·Hex_4·Hep_3·*P*EA_2·*An*Kdo-ol
			1008.7	2019.4	2020.5	11				*P*Cho·Hex_5·Hep_3·*P*EA_2·*An*Kdo-ol
			1029.4	2061.8	2062.3	4				*P*Cho·HexNAc·Hex_4·Hep_3·*P*EA_2·*An*Kdo-ol
			1037.4	2076.8	2077.6	5				*P*Cho·Gly·Hex_5·Hep_3·*P*EA_2·*An*Kdo-ol
			1057.9	2117.8	2119.4	1				*P*Cho·Gly·HexNAc·Hex_4·Hep_3·*P*EA_2·*An*Kdo-ol
			1089.8	2181.6	2182.7	21				*P*Cho·Hex_6·Hep_3·*P*EA_2·*An*Kdo-ol
			1110.7	2223.4	2224.5	13				*P*Cho·HexNAc·Hex_5·Hep_3·*P*EA_2·*An*Kdo-ol
			1118.7	2239.4	2239.7	7				*P*Cho·Gly·Hex_6·Hep_3·*P*EA_2·*An*Kdo-ol
			1129.6	2261.2	2263.5	2				*P*Cho·HexNAc·Hex_6·Hep_3·*P*EA_2·*An*Kdo-ol
			1139.6	2181.2	2181.5	4				*P*Cho·Gly·HexNAc·Hex_5·Hep_3·*P*EA_2·*An*Kdo-ol
			1191.7	2285.4	2386.6	8				*P*Cho·HexNAc·Hex_6·Hep_3·*P*EA_2·*An*Kdo-ol
			1220.2	2242.4	2443.6	3				*P*Cho·Gly·HexNAc·Hex_6·Hep_3·*P*EA_2·*An*Kdo-ol

[a] Average mass units were used for calculation of molecular mass values based on proposed composition as follows: Hex, 162.14; Hep, 192.17; Kdo, 220.18; *An*Kdo-ol, 222.18; *P*, 79.98; *P*EA, 123.05; HexNAc, 203.91; *P*Cho, 165.05; Gly, 57.05; lipid A-OH, 953.02. The relative abundance was estimated from the area of molecular ion peak relative to the total area (expressed as a percentage). Peaks representing less than 5% of the base peak intensity are not included. [b] The observed *m*/*z* values correspond to spectra from NTHi 1124*lic2A*. [c] The observed *m*/*z* values correspond to spectra from NTHi 1124*lpsA*. All other *m*/*z* values correspond to spectra from NTHi 1124wt. Observed values in 1124*lpsA* and 1124*lic2A* varied ±1.0 Da.

ESI-MS of the O-deacylated samples from 1124wt, 1124*lpsA*, 1124*lic2A*, and 1124*lgtC* revealed abundant molecular peaks corresponding to triply and quadruply deprotonated ions. The MS data indicated the presence of heterogeneous mixtures of glycoforms, consistent with each molecular species containing the conserved *P*EA substituted triheptosyl inner-core moiety attached via a phosphorylated Kdo linked to the O-deacylated lipid A (lipid A-OH). Moreover, subpopulations of glycoforms were observed which differed by 123 Da, indicating LPS substitution with a third *P*EA group. Ions corresponding to glycoforms containing between two and seven glycosyl residues were detected as shown in Table 2.

For 1124wt, triply charged ions were observed at *m*/*z* 908.3/949.3, 962.1/1003.5, 1016.3/1057.1, and 1070.4/1111.3, indicating the presence of *P*Cho·Hex_3·Hep_3·*P*EA_{2-3}·*P*·Kdo·lipid A-OH, *P*Cho·Hex_4·Hep_3·*P*EA_{2-3}·*P*·Kdo·lipid A-OH, *P*Cho·Hex_5·Hep_3·*P*EA_{2-3}·*P*·Kdo·lipid A-OH, and *P*Cho·Hex_6·Hep_3·*P*EA_{2-3}·*P*·Kdo·lipid A-OH, respectively. Also, HexNAc-containing glycoforms were observed at *m*/*z* 1030.1, 1084.2/1125.2, and 1138.0/1178.9, corresponding to *P*Cho·HexNAc·Hex_4·Hep_3·*P*EA_2·*P*·Kdo·lipid A-OH, *P*Cho·HexNAc·Hex_5·Hep_3·*P*EA_{2-3}·*P*·Kdo·lipid A-OH, and *P*Cho·HexNAc·Hex_6·Hep_3·*P*EA_{2-3}·*P*·Kdo·lipid A-OH, respectively. The Hex6 glycoforms were found to be the most abundant from their relative peak intensities. The ESI-MS data indicated significantly restricted populations of glycoforms for the mutant strains. Thus, for strain 1124*lpsA*, triply charged ions were observed at *m*/*z* 853.7/894.7, 907.7/948.8, and 962.0, corresponding to glycoforms *P*Cho·Hex_2·Hep_3·*P*EA_{2-3}·*P*·Kdo·lipid A-OH, *P*Cho·Hex_3·Hep_3·*P*EA_{2-3}·*P*·Kdo·lipid A-OH, and *P*Cho·Hex_4·Hep_3·*P*EA_2·*P*·Kdo·lipid A-OH, respectively. The ESI-MS spectrum of 1124*lic2A* showed triply charged ions at *m*/*z* 908.3/948.4, 962.1/1002.4, and 1016.7 corresponding to *P*Cho·Hex_3·Hep_3·*P*EA_{2-3}·*P*·Kdo·lipid A-OH, *P*Cho·Hex_4·Hep_3·*P*EA_{2-3}·*P*·Kdo·lipid A-OH, and *P*Cho·Hex_5·Hep_3·*P*EA_2·*P*·Kdo·lipid A-OH, respectively. In the ESI-MS spectrum of 1124*lgtC*, triply charged ions at *m*/*z* 853.7/894.7, 908.3/949.3, and 962.1/1003.5 corresponded to *P*Cho·Hex_2·Hep_3·*P*EA_{2-3}·*P*·Kdo·lipid A-OH, *P*Cho·Hex_3·

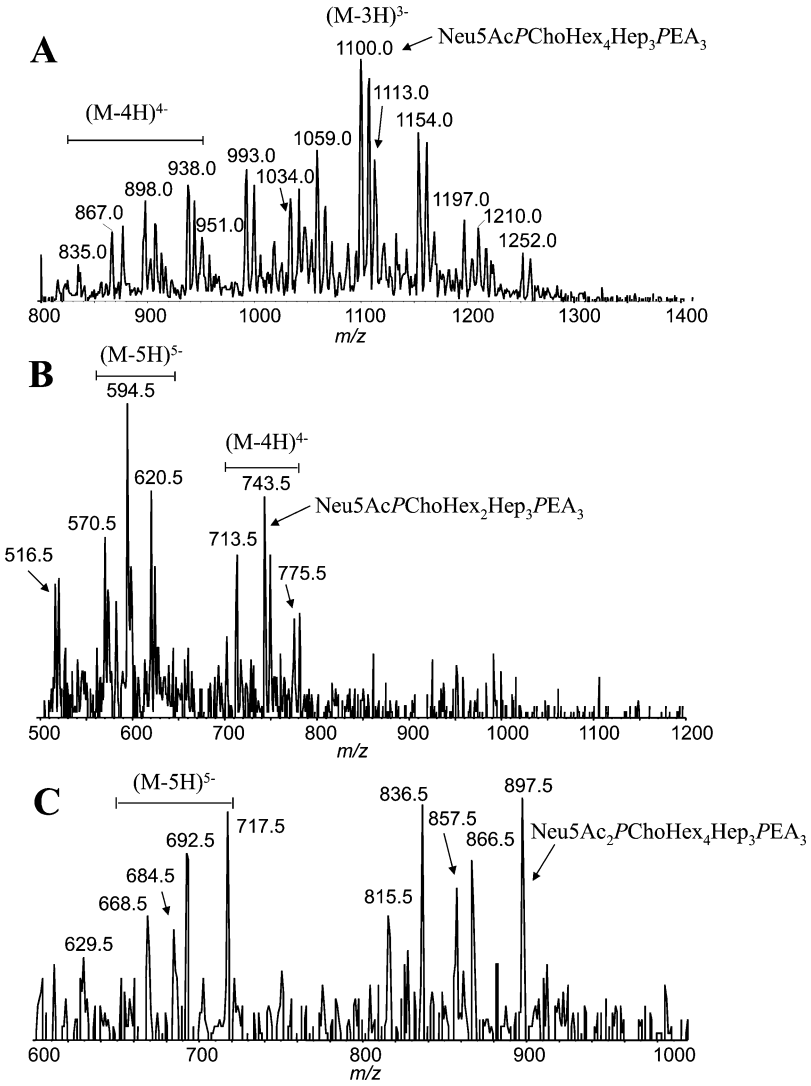

FIGURE 2: CE-ESI-MS/MS (negative mode) spectra of LPS-OH derived from NTHi 1124wt and 1124*lpsA*. The indicated compositions include the *P*·Kdo·lipid A-OH element. (A) Precursor ion spectrum using *m*/*z* 290 as the fragment ion for identification of sialylated components in 1124wt. (B) Precursor ion spectrum using *m*/*z* 290 as the fragment ion for identification of sialylated components in 1124*lpsA*. (C) Precursor ion spectrum using *m*/*z* 581 as the fragment ion for identification of disialylated components in 1124*lgtC*.

Hep_3·PEA_{2-3}·*P*·Kdo·lipid A-OH, and *P*Cho·Hex_4·Hep_3·PEA_{2-3}·*P*·Kdo·lipid A-OH, respectively. From the relative peak intensities in the spectra, it could be concluded that Hex3, Hex3/Hex4, and Hex4 glycoforms were the most abundant species in 1124*lpsA*, 1124*lic2A*, and 1124*lgtC*, respectively.

Ions corresponding to sialylated glycoforms were not unambiguously identified in the full ESI-MS spectra of LPS-OH samples due to extensive overlap with those corresponding to major, nonsialylated glycoforms, and/or low abundances. However, their presence could be confirmed in precursor ion monitoring tandem mass spectrometry experiments (negative ion mode) by scanning for loss of *m*/*z* 290 (Neu5Ac) following CE-ESI-MS/MS. The data are shown in Figure 2 and summarized in Table 3. Quadruply and triply charged ions corresponding to a complex mixture of sialylated glycoforms containing two to five hexose residues were observed in the spectrum of 1124wt (Figure 2A). The major ion at *m*/*z* 1100 corresponded to glycoform Neu5Ac·*P*Cho·Hex_4·Hep_3·PEA_3·*P*·Kdo·lipid A-OH. In addition, ions at *m*/*z* 993, 1034, 1197, and 1252 corresponded to disialylated Hex2, Hex4, and Hex5 glycoforms having the respective compositions, $Neu5Ac_2$·Hex_2·Hep_3·PEA_{2-3}·*P*·Kdo·lipid A-OH, $Neu5Ac_2$·*P*Cho·Hex_4·Hep_3·PEA_3·*P*·Kdo·lipid A-OH, and $Neu5Ac_2$·*P*Cho·Hex_5·Hep_3·PEA_3·*P*·Kdo·lipid A-OH. The spectrum of 1124*lpsA* (Figure 2B) revealed ions corresponding to sialylated Hex2 glycoform $Neu5Ac_1$·*P*Cho·Hex_2·Hep_3·PEA_{2-3}·*P*·Kdo·lipid A-OH. In addition, the disialylated glycoform lacking the phosphorylcholine moiety, $Neu5Ac_2$·Hex_2·Hep_3·PEA_3·*P*·Kdo·lipid A-OH, was identified at *m*/*z* 775.4. The precursor ion scan spectrum of 1124*lgtC* was dominated by ions corresponding to disialylated Hex4 glycoforms having the structures $Neu5Ac_2$·*P*Cho·Hex_4·Hep_3·PEA_{1-3}·*P*·Kdo·lipid A-OH. Disialylated glycoforms in 1124*lpsA* and 1124*lgtC* (Figure 2C) were confirmed by scanning for loss of *m*/*z* 581 (Neu5Ac-Neu5Ac).

Characterization of Lipid A. The lipid A backbone of *H. influenzae* LPS has been shown to consist of a β-1,6-linked D-glucoseamine disaccharide, which is phosphorylated at positions 1 and 4′ (*43*). The disaccharide is primarily acylated with four 3-hydroxytetradecanoic acids. N-Acylation occurs at C2 and C2′ and O-acylation at C3 and C3′. In addition, the 3-hydroxy groups of the fatty acids at positions 2′ and 3′ are acylated with myristic acids (*43*). ESI-MS data (Table

Table 3: Negative Ion ESI-MS Data and Proposed Compositions for Sialylated O-Deacylated LPS (LPS-OH) Based on a Precursor Ion Scan (*m*/*z* 290 and 581) of Nontypeable *H. influenzae* Strains 1124*lpsA*, 1124*lgtC*, and 1124wt[a]

	observed ion (*m*/*z*)				molecular mass (Da)		
sample	$(M-6H)^{6-}$	$(M-5H)^{5-}$	$(M-4H)^{4-}$	$(M-3H)^{3-}$	observed	calculated	proposed composition
lpsA		570.5	713.5		2857.8	2856.4	Neu5Ac·*P*Cho·Hex_2·Hep_3·PEA_2
		594.5	743.5		2977.8	2979.4	Neu5Ac·*P*Cho·Hex_2·Hep_3·PEA_3
	516.5[b]	620.5	775.5		3106.2	3105.6	Neu$5Ac_2$·Hex_2·Hep_3·PEA_3
lgtC		634.5	794.5		3179.8	3180.7	Neu5Ac·*P*Cho·Hex_4·Hep_3·PEA_2
		652.5[b]	815.5		3266.8	3267.7	Neu$5Ac_2$·Hex_3·Hep_3·PEA_3
		659.5	825.5		3304.3	3303.8	Neu5Ac·*P*Cho·Hex_4·Hep_3·PEA_3
		668.5[b]	836.5		3348.8	3349.0	Neu$5Ac_2$·*P*Cho·Hex_4·Hep_3·*P*EA
		684.5[b]	857.5		3430.8	3429.8	Neu$5Ac_2$·Hex_4·Hep_3·PEA_3
		693.5[b]	866.5		3471.3	3472.0	Neu$5Ac_2$·*P*Cho·Hex_4·Hep_3·PEA_2
		717.5[b]	898.5		3595.3	3595.1	Neu$5Ac_2$·*P*Cho·Hex_4·Hep_3·PEA_3
wt				951	2856	2856.4	Neu5Ac·*P*Cho·Hex_2·Hep_3·PEA_2
				993	2982	2979.4	Neu5Ac·*P*Cho·Hex_2·Hep_3·PEA_3
				993	2982	2982.4	Neu$5Ac_2$·Hex_2·Hep_3·PEA_2
				1006	3021	3018.5	Neu5Ac·*P*Cho·Hex_3·Hep_3·PEA_2
				1034	3105	3105.6	Neu$5Ac_2$·Hex_2·Hep_3·PEA_3
				1047	3144	3141.6	Neu5Ac·*P*Cho·Hex_2·Hep_3·PEA_3
				1059	3180	3180.7	Neu5Ac·*P*Cho·Hex_4·Hep_3·PEA_2
				1100	3303	3303.8	Neu5Ac·*P*Cho·Hex_4·Hep_3·PEA_3
			835	1113	3343	3342.8	Neu5Ac·*P*Cho·Hex_5·Hep_3·PEA_2
			—[c]	1154	3465	3465.9	Neu5Ac·*P*Cho·Hex_5·Hep_3·PEA_3
			867	—[c]	3472	3472.0	Neu$5Ac_2$·*P*Cho·Hex_4·Hep_3·PEA_2
			898	1197	3595	3595.1	Neu$5Ac_2$·*P*Cho·Hex_4·Hep_3·PEA_3
			938	1252	3758	3757.2	Neu$5Ac_2$·*P*Cho·Hex_5·Hep_3·PEA_3

[a] Average mass units were used for calculation of molecular mass values based on proposed compositions as follows: Hex, 162.14; HexNAc, 203.19; Hep, 192.17; Kdo, 220.18; *P*, 79.98; *P*Ea, 123.05; *P*Cho, 165.13; Neu5Ac, 291.26; lipid A-OH, 953.02. All compositions include the *P*·Kdo·lipid A-OH element. [b] Confirmed in a precursor ion scan on *m*/*z* 581. [c] Not detected due to overlap.

Table 4: Methylation Analysis Data of the Dephosphorylated[a] OS Samples Derived from *H. influenzae* 1124wt, 1124*lpsA*, 1124*lic2A*, and 1124*lgtC*

			relative abundance			
methylated sugar[b]	T_{gm}[c]	linkage assignment	1124wt	1124*lpsA*	1124*lic2A*	1124*lgtC*
2,3,4,6-Me_4-Glc	1.00	D-Glc*p*-(1-		trace	10	4
2,3,4,6-Me_4-Gal	1.06	D-Gal*p*-(1-	15	18	13	28
2,3,6-Me_3-Gal	1.24	-4)-D-Gal*p*-(1-	13	16	11	
2,3,6-Me_3-Glc	1.26	-4)-D-Glc*p*-(1-	17	12	17	27
2,4,6-Me_3-Gal	1.29	-3)-D-Gal*p*-(1-	2			
2,3,4,6,7-Me_4-Hep	1.43	L,D-Hep*p*-(1-	2	19	2	?
3,4,6,7-Me_4-Hep	1.65	-2)-L,D-Hep*p*-(1-	30	20	22	19
2,6,7-Me_3-Hep	1.76	-3,4)-L,D-Hep*p*-(1-	19	16	14	19
4,6,7-Me_3-Hep	1.86	-2,3)-L,D-Hep*p*-(1-	3		11	3

[a] Methylation analysis data obtained from OS samples that were not dephosphorylated also showed the presence of terminal GalNAc. [b] 2,3,4,6-Me_4-Glc represents 1,5-di-*O*-acetyl-2,3,4,6-tetra-*O*-methyl-D-glucitol-1-d_1, etc. [c] Retention times (T_{gm}) are reported relative to that of 2,3,4,6-Me_4-Glc.

2), fatty acid compositional analysis yielding 3-hydroxytetradecanoic acid, and NMR experiments (data not shown) on LPS-OH were indicative of this lipid A structural model. Moreover, ESI-MS of the lipid A derived from 1124wt, purified by partitioning in chloroform, methanol, and water (2:1:1; v/v/v), in the negative mode with chloroform and methanol (1:1; v/v) as solvent (*46*) revealed major ions at *m*/*z* 1825.0 and 1744.6 corresponding to diphosphorylated and monophosphorylated lipid A, respectively, with four 3-hydroxytetradecanoic acid and two tetradecanoic acids. The monophosphorylated lipid A is assumed to be a product of the mild acid hydrolysis method described below.

Characterization of Oligosaccharides Derived from 1124wt and Isogenic lpsA, lic2A, and lgtC Mutants. Mild acid hydrolysis of LPS with dilute aqueous acetic acid afforded insoluble lipid A and core oligosaccharide material (OS), which after purification by gel filtration chromatography resulted in oligosaccharide samples OS1124wt, OS1124*lpsA*, OS1124*lic2A*, and OS1124*lgtC*. Sugar analysis of the OS (Table 1) was consistent with data obtained for the corresponding LPS-OH samples revealing the presence of Glc, Gal, and Hep in all four strains and GalN in all strains except 1124*lgtC*. The absence of GlcN in the OS samples confirmed this sugar to be part of only lipid A.

OS samples were dephosphorylated with 48% hydrogen fluoride prior to methylation analysis. The resulting material from OS1124wt revealed terminal Gal, 4-substituted Gal, 4-substituted Glc, 2-substituted Hep, and 3,4-disubstituted Hep in a 15:13:17:30:19 proportion as the major constituents (Table 4). Methylation analysis of dephosphorylated OS1124*lpsA* showed a terminal Hep as a major component in addition to these sugars which is in agreement with the expected lack of substitution of HepIII. OS1124*lic2A* and OS1124*lgtC* contained the same sugars as OS1124wt except that terminal Glc was also observed in significant amounts in OS1124*lic2A*, while 4- and 3-substituted Gal were not observed in OS1124*lgtC*. It is noteworthy that OS1124*lic2A* contained 4-substituted Gal. The methylation analysis data

were consistent with biantennary structures, containing the common inner-core element, L-α-D-Hep*p*-(1→2)-L-α-D-Hep*p*-(1→3)-[*β*-D-Glc*p*-(1→4)]-L-α-D-Hep*p*-(1→5)-α-Kdo*p*, of *H. influenzae* LPS.

ESI-MS on OS samples (Table 2) indicated all four strains to be glycylated. The Hex6-, Hex3-, Hex3/Hex4-, and Hex4-containing glycoforms were prevalent in1124wt, 1124*lpsA*, 1124*lic2A*, and 1124*lgtC*, respectively. All of the strains comprised an anhydro-Kdo moiety (*An*Kdo-ol) formed during delipidation by *β*-elimination of a *PP*EA group from C4 of Kdo as observed in previous studies (*4*−*6*, *8*−*10*, *12*, *13*, *16*−*21*).

In the ESI-MS spectrum of OS1124wt (negative mode), doubly charged ions were observed at *m*/*z* 847.3, 927.9, 1008.7.0, and 1089.8, corresponding to glycoforms *P*Cho·Hex_{3-6}·Hep_3·*P*EA_2·*An*Kdo-ol, respectively. Their glycylated counterparts were detected at *m*/*z* 875.3, 956.9, 1037.4, and 1118.7, respectively. HexNAc-containing glycoforms were identified at *m*/*z* 1029.4, 1110.7, and 1129.6 which corresponded to *P*Cho·HexNAc·Hex_{4-6}·Hep_3·*P*EA_2·*An*Kdo-ol, respectively. Glycylated HexNAc glycoforms were found at *m*/*z* 1057.9, 1139.6, and 1220.2, corresponding to *P*Cho·Gly·HexNAc·Hex_{4-6}·Hep_3·*P*EA_2·*An*Kdo-ol, respectively. ESI-MS on OS1124*lpsA* revealed the *P*Cho·Hex_{1-4}·Hep_3·*P*EA_2·*An*Kdo-ol glycoforms at *m*/*z* 684.2, 765.4, 846.1, and 925.9, respectively. The glycylated counterparts were found at *m*/*z* 712.7, 793.4, 874.5, and 955.9, respectively. ESI-MS on OS1124*lic2A* revealed ions at *m*/*z* 765.5, 847.3, and 927.9 corresponding to *P*Cho·Hex_{2-4}·Hep_3·*P*EA_2·*An*Kdo-ol, respectively. The ions found at *m*/*z* 742.6, 794.0, 823.0, 875.3, 904.7, and 956.9 corresponded to glycylated glycoforms. Notably, *m*/*z* 742.6, 823.0, 906.5, and 985.0 corresponded to glycoforms with two glycines, whereas the others contained one glycine. The ions at *m*/*z* 765.1, 847.1, and 928.1 in the ESI-MS spectrum of OS1124*lgtC* revealed that the sample comprised *P*Cho·Hex_{2-4}·Hep_3·*P*EA_2·*An*Kdo-ol glycoforms, respectively. Glycoforms containing one glycine were found at *m*/*z* 794.9, 875.3, and 956.3, while their counterparts with two glycines were identified at *m*/*z* 823.0, 906.5, and 985.0.

Information about the location of Gly, phosphorylation sites, and the glycose sequence of the *P*Cho·Gly·Hex_3·Hep_3·*P*EA_2·*An*Kdo-ol component in OS1124*lpsA* was provided by CE-ESI-MS/MS in the positive mode. A product ion spectrum was obtained from its doubly charged ion at *m*/*z* 877. Ions at *m*/*z* 1382 and 1102 corresponded to losses of Gly·Hep·*P*EA and Hex_3·*P*Cho units from the molecular ion, respectively. The ion at *m*/*z* 328 corresponded to *P*Cho·Hex to which additions corresponding to HexHex (*m*/*z* 490 and 652) or Hep (*m*/*z* 520) could be made, the latter indicating that *P*Cho·Hex substituted for HepI. In addition, the ion at *m*/*z* 373 corresponded to a Gly·Hep·*P*EA fragment. It could be concluded that glycine and one *P*EA residue were linked to HepIII.

Sequence Analysis of Dephosphorylated and Permethylated Oligosaccharide Samples by Multiple-Step MS (MS^n). OS1124wt, OS1124*lpsA*, OS1124*lic2A*, and OS1124*lgtC* were dephosphorylated, permethylated, and analyzed by ESI-MS^n to determine the sequence and branching details of the various glycoforms. This strategy has been proven to be particularly informative for profiling glycoform expression in several NTHi strains (*18*−*20*, *23*). For most glycoforms, the presence of several isomeric compounds was revealed by identifying product ions in MS^2 spectra (Table 5). Only isomeric glycoforms showing chain elongation from HepI and/or HepIII were identified, consistent with the absence of *lic2C* as indicated by genomic analysis (data not shown). MS^3 experiments were employed when necessary to confirm structures. Because of the increased MS response obtained by permethylation in combination with added sodium acetate, several glycoforms were observed in the MS spectra that were not detected in underivatized samples (Figure 3). Thus, in the ESI-MS spectrum of dephosphorylated and permethylated OS1124*lpsA* (positive mode, Figure 3B), five sodiated adduct ions ([M + Na^+]) were observed at *m*/*z* 1263.7, 1468.3, 1671.8, 1875.9, and 1916.7 corresponding to permethylated Hex_{1-4}·Hep_3·*An*Kdo-ol and HexNAc·Hex_3·Hep_3·*An*Kdo-ol, respectively. To obtain sequence and branching information, these molecular ions were further fragmented in MS^2 and MS^3 experiments. The Hex1 glycoform was defined by ions at *m*/*z* 1001.6 and 753.5 corresponding to a loss of a tHep-Hep unit from the parent ion (*m*/*z* 1263.7). The Hex2 glycoform was defined by ions at *m*/*z* 1205.7 and 957.6 corresponding to the loss of tHep-Hep from the parent ion (*m*/*z* 1468.3). The Hex3 glycoform was defined by ions at *m*/*z* 1409.7 and 1161.6 corresponding to the loss of tHep-Hep from the parent ion (*m*/*z* 1671.8). The Hex4 glycoform was defined by ions at *m*/*z* 1613.9 and 1161.6 corresponding to the loss of tHep-Hep from the parent ion (*m*/*z* 1875.9). MS^2 fragmentation on the ion at *m*/*z* 1916.7 corresponding to the HexNAc·Hex_3·Hep_3·*An*Kdo-ol glycoform resulted, inter alia, in signals at *m*/*z* 1655.0 corresponding to the loss of tHep (Figure 4A). We subjected *m*/*z* 1655.0 to further fragmentation which resulted in an ion at *m*/*z* 1406.8, corresponding to the loss of -HepII- (Figure 4B). In the subsequent MS^4 fragmentation of *m*/*z* 1406.8, the resulting ions at *m*/*z* 1147.5, 943.0, and 740.3 corresponded to the loss of tHexNAc, tHexNAc·Hex, and tHexNAc·Hex-Hex, respectively, indicating a tHexNAc·Hex-Hex-Hex unit linked to HepI (Figure 4C). In summary, in OS1124*lpsA* chain elongation only occurred from HepI which was in agreement with the proposed function of the *lpsA* gene.

In the ESI-MS spectrum of OS1124*lic2A* (positive mode, Figure 3C), six sodiated adduct ions were observed at *m*/*z* 1264.7, 1468.2, 1672.0, 1875.6, 2079.4, and 2121.6 corresponding to permethylated Hex_{1-5}·Hep_3·*An*Kdo-ol and HexNAc·Hex_4·Hep_3·*An*Kdo-ol glycoforms, respectively. These ions were further fragmented in MS^2 experiments, and some of the resulting product ions underwent further fragmentation to confirm the existence of the proposed glycoforms shown in Table 5. One isomeric Hex1 glycoform was defined by the ion at *m*/*z* 797.4 corresponding to the loss of tHex-Hep from the parent ion (*m*/*z* 1264.7). The other Hex1 glycoform was defined by the ion at *m*/*z* 753.5 corresponding to a loss of a tHep-Hep unit from the parent ion. Two Hex2 isomeric glycoforms were identified by MS^2 on the molecular ion at *m*/*z* 1468.2 and subsequent MS^3 on the product ions at *m*/*z* 1205.6 and 1001.5 representing the loss of tHep and tHex-Hep, respectively. The isomer having a disaccharide linked to HepI was defined by the ion at *m*/*z* 957.5 corresponding to the loss of HepII from *m*/*z* 1001.5. The isomer having a hexose linked to HepI was defined by the ion at *m*/*z* 753.5 corresponding to the loss of -HepIII-HepII from *m*/*z* 1205.6. Two Hex3 isomers were identified by performing MS^2 on

Table 5: Structures of Glycoforms from OS1124wt, OS1124*lpsA*, OS1124*lic2A*, and OS1124*lgtC* Elucidated by ESI-MS^n (Subscripts Denoted by the Letters *a*−*d* Indicate the Number of Hexose Residues in the Following Structure)

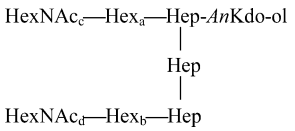

	relative abundance,[a] (%)				structure 1124wt				structure *lpsA*			structure *lic2A*			structure *lgtC*		relative abundance[b]			
glycoform	wt	*lpsA*	*lic2A*	*lgtC*	*a*	*b*	*c*	*d*	*a*	*b*	*c*	*a*	*b*	*c*	*a*	*b*	wt	*lpsA*	*lic2A*	*lgtC*
Hex_1	5	4	4		1	0	0	0	1	0	0	1	0	0			M	H	M	
					0	1	0	0				0	1	0			M		M	
Hex_2	5	19	15	7	2	0	0	0	2	0	0	2	0	0	2	0	H	H	M	M
					1	1	0	0				1	1	0	1	1	L		M	L
					0	2	0	0							0	2	L			L
Hex_3	8	67	33	20	3	0	0	0	3	0	0	3	0	0			M	H	M	
					2	1	0	0				2	1	0	2	1	L		M	M
					1	2	0	0							1	2	L			M
Hex_4	11	6	40	72	4	0	0	0	4	0	0	4	0	0			L	H	H	
					3	1	0	0									L			
					2	2	0	0							2	2	M			H
					1	3	0	0									L			
Hex_5	15		6									5	0	0					H	
					4	1	0	0									L			
					3	2	0	0									M			
					2	3	0	0									M			
Hex_6	16				4	2	0	0									L			
					3	3	0	0									H			
HexNAc-Hex_3	4	5			3	0	1	0	3	0	1						M	H		
					0	3	0	1									M			
HexNAc-Hex_4	6		3		3	1	1	0				3	1	1	0				H	
					1	3	0	1									H			
HexNAc-Hex_5	8				2	3	0	1									H			
HexNAc-Hex_6	13				3	3	0	1									H			
					3	3	1	0									L			
$HexNAc_2$-Hex_6	6				3	3	1	1									H			

[a] Relative abundance for each glycoform. Calculated from the intensity of the molecular ion peak relative to the total intensity of all molecular ion peaks in the MS spectrum expressed as a percentage. [b] Relative abundance for structural isomers of each glycoform. Calculated from the intensity of the product ions in the MS^2 spectrum and indicated as follows: H, high (>80%); M, medium (30−80%); L, low (2−30%); and T, trace (<2%).

the parent ion at *m*/*z* 1672.0 and subsequent MS^3 on the resulting product ions at *m*/*z* 1409.7 and 1205.6 due to the loss of tHep and tHex-Hep, respectively. The isomeric glycoform having a trisaccharide substituting for HepI was defined by the ion at *m*/*z* 1161.5 observed in the MS^3 spectrum at *m*/*z* 1409.7 (loss of tHep-Hep). MS^3 of the ion at *m*/*z* 1205.6 showed a product ion at *m*/*z* 957.4 (loss of -HepII-) defining the Hex3 isomer with a disaccharide substituted for HepI. Only one Hex4 glycoform was identified when MS^2 was performed on the molecular ion at *m*/*z* 1875.6 and subsequent MS^3 on the product ion due to the loss of -Hex-HepIII at *m*/*z* 1409.6. The resulting product ion at *m*/*z* 1161.4 showed the loss of -HepII- and thus evidenced a trisaccharide group linked to HepI. Only one Hex5 glycoform was identified by MS^2 on the molecular ion at *m*/*z* 2079.4 and MS^3 on the product ion due to the loss of -Hex-HepIII at *m*/*z* 1614.0. The ion at *m*/*z* 1366.0 showing the loss of -HepII indicated that a tetrasaccharide group was linked to HepI. The structure of the HexNAc·Hex_4·Hep_3·*An*Kdo-ol glycoform was determined by MS^2 on the molecular ion at *m*/*z* 2121.5 and subsequent MS^3 on the ion at *m*/*z* 1407.4 due to the loss of Hex-Hep-Hep. The resulting ions at *m*/*z* 1148.5 and 944.8 were due to the loss of tHexNAc and tHexNAc·Hex, respectively, evidencing a tHexNAc·Hex-Hex-Hex unit linked to HepI. The function of the *lic2A* gene in strain 1124 was confirmed since glycoforms with chain extension from Hex-HepIII were not detected by ESI-MS^n.

In the ESI-MS spectrum of OS1124*lgtC* (Figure 3D), major ions were observed at *m*/*z* 1468.1, 1671.9, and 1876.8 corresponding to permethylated Hex_{2-4}·Hep_3·*An*Kdo-ol glycoforms, respectively. In analogy with the experiments described for OS1124*lpsA* and OS1124*lic2A*, MS^2 on these ions and subsequent MS^3 on product ions (data not shown) led to the identification of six glycoforms in 1124*lgtC* (Table 5), most of which showed disaccharide substitution at HepI and/or HepIII.

In the ESI-MS spectrum of OS1124wt (Figure 3A), major ions were observed at *m*/*z* 1264.0, 1468.1, 1671.9, 1875.9, 2079.8, 2284.4, and 2528.9 corresponding to permethylated Hex_{2-6}·Hep_3·*An*Kdo-ol. Minor HexNAc-containing glycoforms were observed at *m*/*z* 1917.0, 2121.8, 2324.3, and 2528.9 corresponding to HexNAc·Hex_{3-6}·Hep_3·*An*Kdo-ol, respectively, as well as an ion corresponding to $HexNAc_2$·Hex_6·Hep_3·*An*Kdo-ol at *m*/*z* 2775.0. These ions were further fragmented in MS^2 experiments, and some of the resulting product ions underwent further fragmentation (data not shown) to confirm the existence of the proposed glycoforms shown in Table 5. The results of OS1124wt reflected those obtained from the *lpsA*, *lic2A*, and *lgtC* mutants showing full extensions from HepI by HexNAcHexHexHexHex or Hex4 units and from HepIII by a HexNAcHexHexHex unit.

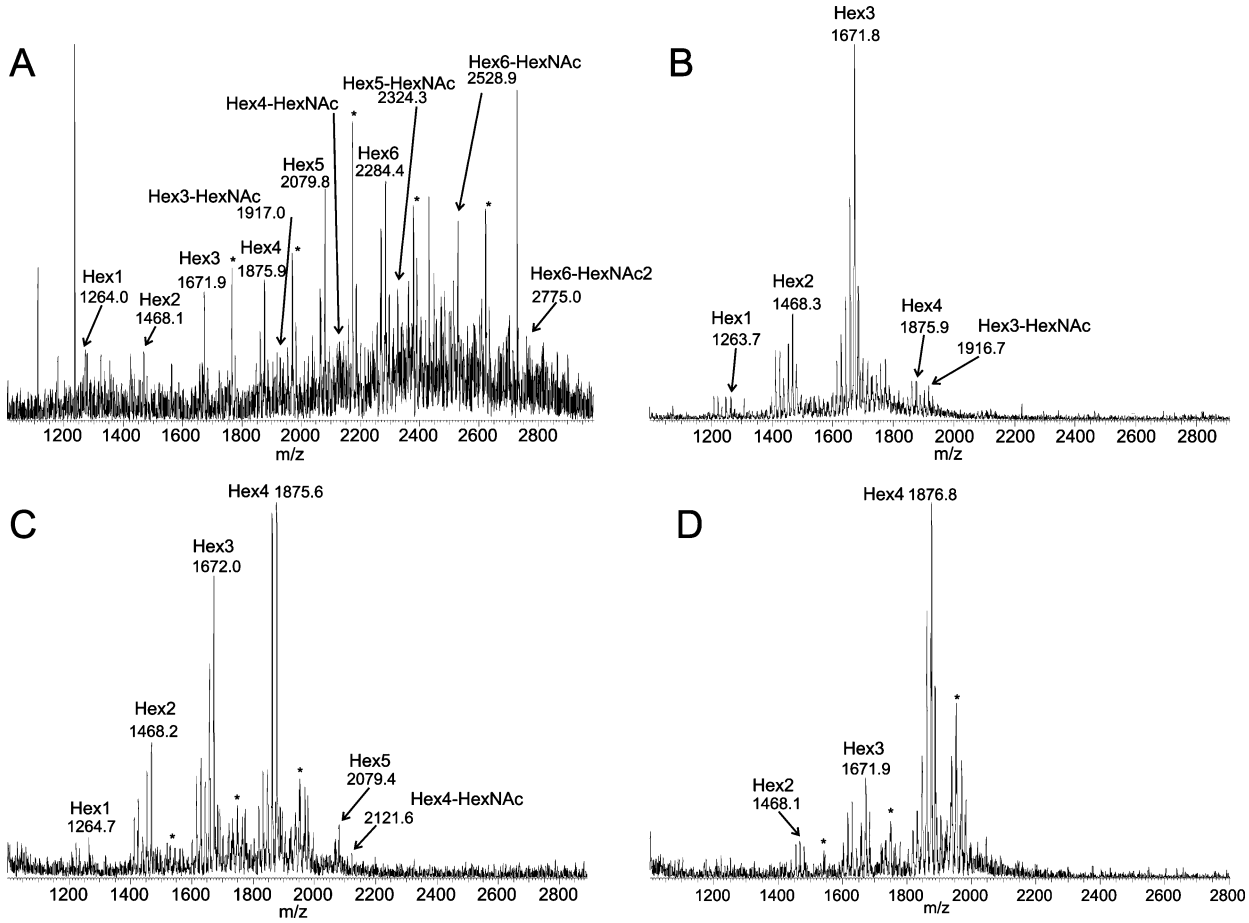

FIGURE 3: ESI-MS spectra showing sodiated adducts $(M + Na)^+$ of permethylated (A) OS1124wt, (B) OS1124*lpsA*, (C) OS1124*lic2A*, and (D) OS1124*lgtC*. The peaks denoted with asterisks indicate glycoforms with monomethylated phosphate groups resulting from incomplete dephosphorylation.

NMR Analysis of OS1124wt, OS1124lpsA, OS1124lic2A, and OS1124lgtC. The structures of major oligosaccharides derived from the various strains were elucidated by detailed ^{1}H and ^{13}C NMR analyses. ^{1}H and ^{13}C NMR resonances were assigned using gradient chemical shift correlation techniques (COSY, phase-sensitive TOCSY, HMQC, phase-sensitive HSQC, and HMBC experiments). The chemical shift data corresponding to OS1124wt, OS1124*lpsA*, OS1124*lic2A*, and OS1124*lgtC* are given in Table 6. Subspectra corresponding to the individual glycosyl residues were identified on the basis of spin connectivity pathways delineated in the ^{1}H chemical shift correlation maps, the chemical shift values, and the vicinal coupling constants.

The chemical shift data are consistent with each D-sugar residue being present in the pyranosyl ring form. Further evidence for this conclusion was obtained from NOE data which also served to confirm the anomeric configurations of the linkages and the monosaccharide sequence. The Hep ring systems were identified on the basis of the small $J_{1,2}$ values, and their α-configurations were confirmed by the occurrence of single intraresidue NOEs between the respective H1 and H2 resonances. Several signals for methylene protons of *An*Kdo-ol were observed in the COSY and TOCSY experiments, and this is due to the fact that several anhydro forms of Kdo are formed during the hydrolysis by elimination of phosphate or pyrophosphoethanolamine from the C4 position (*5*).

Structure of the Hex3 Glycoform in OS1124lpsA. Sequence analysis of OS1124*lpsA* by ESI-MS^n revealed a predominant Hex3 glycoform having a triheptosyl inner core from which chain elongation by a trisaccharide unit only appeared from HepI (see above and Table 5). In the ^{1}H NMR spectrum of OS1124*lpsA*, anomeric resonances corresponding to the triheptosyl moiety (HepI−HepIII) were identified at δ 5.04−5.12, 5.85−5.90, and 5.23, respectively (Figure 5). Interresidue NOE connectivities between proton pairs HepIII H1/HepII H2 and HepII H1/HepI H3 established the presence of the common inner-core triheptosyl moiety of *H. influenzae*. Subspectra corresponding to the hexose residues were identified in the two-dimensional COSY and TOCSY spectra at δ 5.00 (Gal residue VI), 4.64 (Gal residue V), and 4.57 (Glc residue IV) (Figure 6A). The chemical shift data were consistent with VI being a terminal residue in agreement with methylation analysis. The presence of the globoside trisaccharide attached to HepI, with the sequence α-D-Gal*p*-(1→4)-β-D-Gal*p*-(1→4)-β-D-Glc*p*-(1→4)-L-α-D-Hep*p*-(1→, was confirmed by interresidue NOEs between VI H1 and V H4, V H1 and IV H4, and IV H1 and HepI H4 and H6 (Figures 6B and 7).

As observed previously, HepII H6 of the inner core was detected in the β-anomeric region at δ 4.57. The signal at δ 4.57 correlated to δ 75.4 in the ^{1}H−^{13}C HMQC spectrum which was in agreement with previous data (*4*−*6*, *8*−*10*,

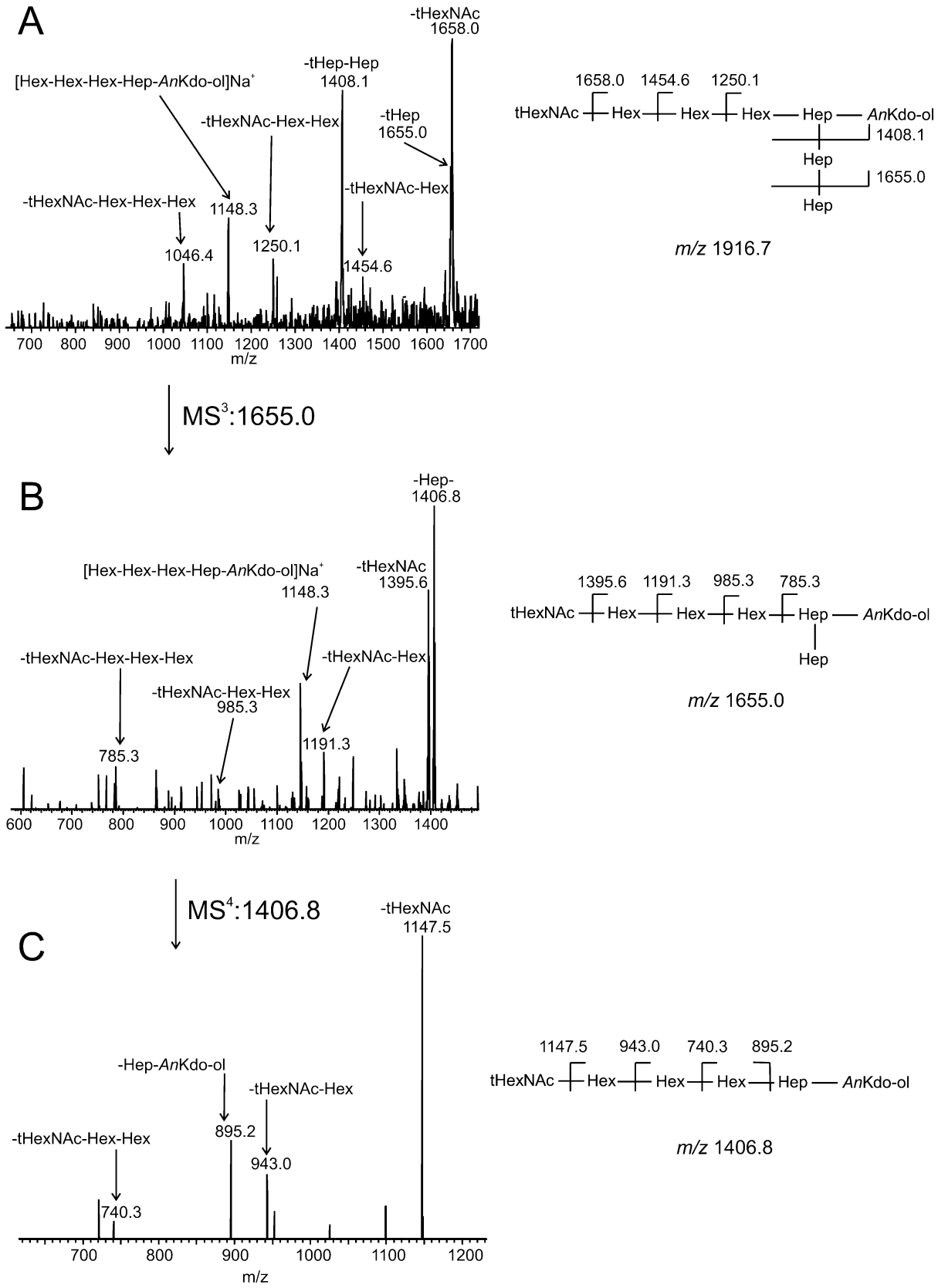

FIGURE 4: ESI-MS^n analysis of permethylated OS1124*lpsA*-P. (A) MS^2 spectrum of *m*/*z* 1916.7 corresponding to the sodium adduct of the Hex3·HexNAc glycoform. (B) MS^3 spectrum of the fragment ion at *m*/*z* 1655.0. (C) MS^4 spectrum of the fragment ion at *m*/*z* 1406.8.

12, *13*, *16*−*21*). ^{1}H−^{31}P correlation studies demonstrated *P*EAI to be linked to O6 of HepII as a ^{31}P resonance at δ 0.73 correlated to the methylene protons of *P*EAI at δ 4.12 and to H6 of HepII at δ 4.57. Furthermore, these studies indicated that *P*EAII was substituted at the O3 position of HepIII since a ^{31}P resonance at δ 0.04 coupled to the methylene protons of *P*EAII at δ 4.14 and to H3 of HepIII at δ 4.36. This finding was corroborated by the significantly

Table 6: ^{1}H and ^{13}C NMR Chemical Shifts for NTHi 1124*lpsA*, 1124*lic2A*, 1124*lgtC*, and 1124wt Recorded in D_2O at 22, 25, 22, and 30 °C, Respectively[a]

Residue	Glycose unit	H-1/C-1	H-2/C-2	H-3/C-3	H-4/C-4	H-5/C-5	H-6_A/C-6	H-6_B	H-7_A/C-7	H-7_B
Hex3 glycoform (1124*lpsA*)										
I	→3, 4)-L-α-D-Hep*p*(1→	5.04 (n.r.)	3.99	3.97[b]	4.29	-[a]	4.11[d]		-[a]	-[a]
		97.5	71.1	72.7[c]	74.5		69.0			
II	L-α-D-Hep*p*(1→	5.86[e] (n.r.)	4.26	-[a]	-[a]	3.90	4.57		3.75	3.92
	6	99.3	79.8			-[a]	75.4		61.0	
	↑									
	*P*EA									
III	→2)-L-α-D-Hep*p*(1→	5.23[f] (n.r)	4.28[h]	4.36	-[a]	-[a]	-[a]		-[a]	
	3	101.9[g]	70.4	76.9[i]						
	↑									
	*P*EA									
IV	→4)-β-D-Glc*p* (1→	4.57 (7.8)	3.46	3.62[j]	3.75	3.74	4.33[l]	4.33[l]		
	6	103.8	73.6	75.5	78.8[k]	74.6	64.5			
	↑									
	*P*Cho									
V	→4)-β-D-Gal*p*(1→	4.64[m] (7.8)	3.54	3.74	4.06	-[a]	-[a]			
		103.9	71.5	73.3	78.2					
VI	α-D-Gal*p*(1→	5.00[n] (4.1)	3.83	3.91	4.04	4.38	3.70	3.70		
		101.3	69.5	70.1	71.6	71.6	63.0			
Hex4 glycoform (derived from 1124*lic2A*)										
VII	β-D-Glc*p* (1→	4.66 (8.3)	3.34	3.56	3.44	3.44	3.73	3.90		
		103.3	73.7	76.3	73.2	76.5	62.1			
Hex4 glycoform (derived from 1124*lgtC*)										
VII	→4)-β-D-Glc*p* (1→	4.73 (8.3)	3.39	3.68	3.66	3.59	3.81	3.99		
		102.8	73.1	74.7	79.7	75.1	60.9			
V	β-D-Gal*p*(1→	4.77[o] (7.8)	3.52	3.65	3.93	-[a]	-[a]			
		103.8	71.8	73.7	69.4					
VIII	β-D-Gal*p*(1→	4.45 (7.8)	3.55	3.70	3.96	-[a]	-[a]			
		104.0	71.8	73.2	69.4					
Hex6 glycoform (derived from 1124wt)										
V	→4)-β-D-Gal*p*(1→	4.86 (7.8)	3.59	3.76	4.07	-[a]	-[a]			
		103.8	71.5	74.2	78.2					
VIII	→4)-β-D-Gal*p*(1→	4.53 (7.8)	3.61	3.78	4.08	3.83				
		104.3	72.2	74.2	78.2	76.2				
IX	α-D-Gal*p*(1→	4.97 (4.2)	3.85	3.94	4.07	4.38	3.74			
		101.3	69.2	70.1	71.1	71.8	63.3			
Hex7 glycoform (derived from 1124wt)										
IX	→3)-α-D-Gal*p*(1→	4.94 (4.4)	3.94	3.98	4.28	-[a]	-[a]			
		101.3	68.7	77.2	69.7					
X	α-D-Gal*p*NAc(1→	4.68 (7.8)	3.97	3.80	3.97	-[a]	-[a]			
		103.8	54.8	64.1	69.0					
***P*EAI**		4.16	3.30							
		63.2	40.8							
***P*EAII**		4.22	3.34							
		62.4	40.8							
***P*Cho**		4.39	3.72							
		60.4	66.9							
Gly			4.01[p]							
			41.4[p]							

[a] $^{3}J_{H,H}$ values for anomeric ^{1}H resonances are given parentheses. n.r. means not resolved (small coupling). Signals corresponding to *P*Cho methyl protons and carbons occurred at 3.16 and 54.8 ppm, respectively. Pairs of deoxy protons of reduced *An*Kdo were identified in the DQF-COSY spectrum at δ 1.89−2.16. -[a] means not determined. Chemical shift values which differ by more than ±0.06 ppm (^{1}H) and ±0.6 ppm (^{13}C) between strains are denoted with superscript letters as follows: [b]4.06^{wt}/4.04^{lic2A}, [c]75.7^{wt}/75.2^{lic2A}/75.0^{lgtC}, [d]4.20^{wt}/4.17^{lic2A}/4.18^{lgtC}, [e]5.70^{wt}/5.69^{lic2A}/5.72^{lgtC}, [f]5.11^{wt}/5.08^{lic2A}/5.11^{lgtC}, [g]100.7^{wt,lgtC}/100.8^{lic2A}, [h]4.40^{wt}/4.36^{lic2A}/4.38^{lgtC}, [i]75.4^{wt,lgtC}/75.3^{lic2A}, [j]3.73^{wt}/3.71^{lic2A}/3.74^{lgtC}, [k]80.8^{wt,lgtC}/80.7^{lic2A}, [l]4.25, 4.38^{wt}/4.22, 4.37^{lic2A}/4.23, 4.36^{lgtC}, [m]4.86^{wt}/4.83^{lic2A}/4.77^{lgtC}, [n]4.95^{wt}, [o]4.74^{wt}, and [p]observed in the 1124*lgtC* mutant.

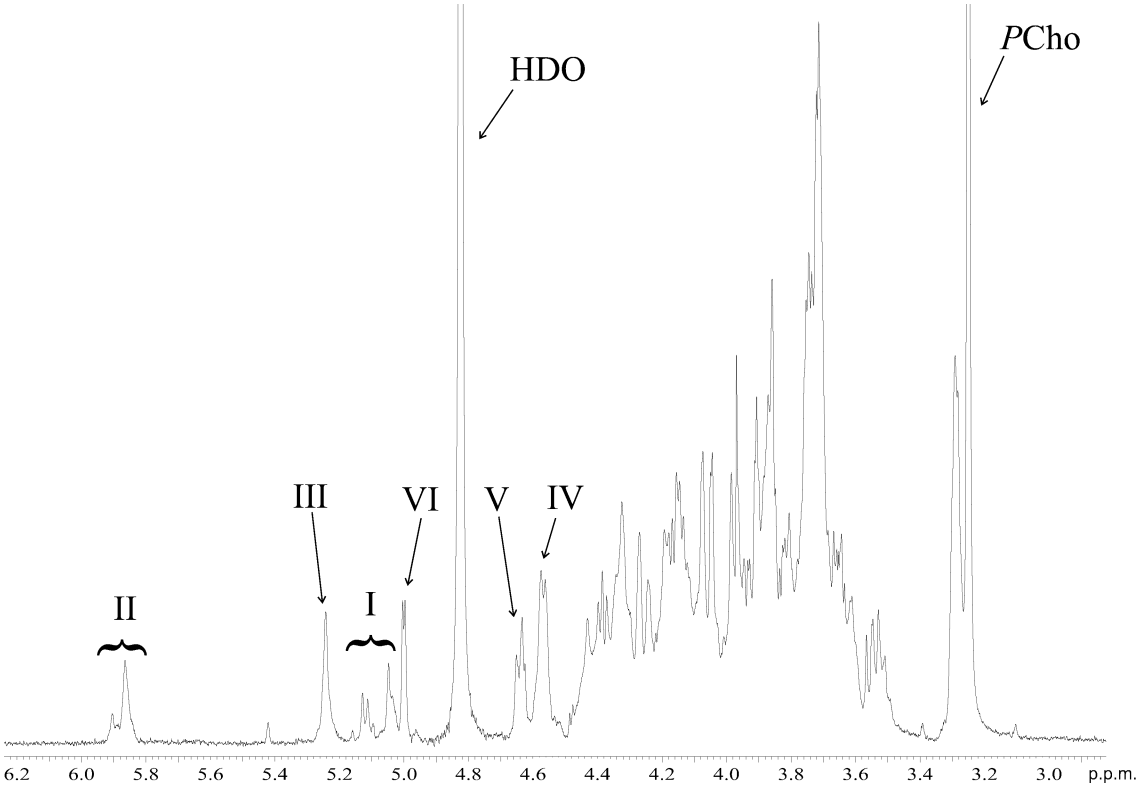

FIGURE 5: ^{1}H NMR spectrum of OS derived from LPS of 1124*lpsA* recorded in D_2O at 22 °C. The anomeric resonances of the major Hex3 glycoform are indicated. See Table 6 for an explanation of the Roman numerals.

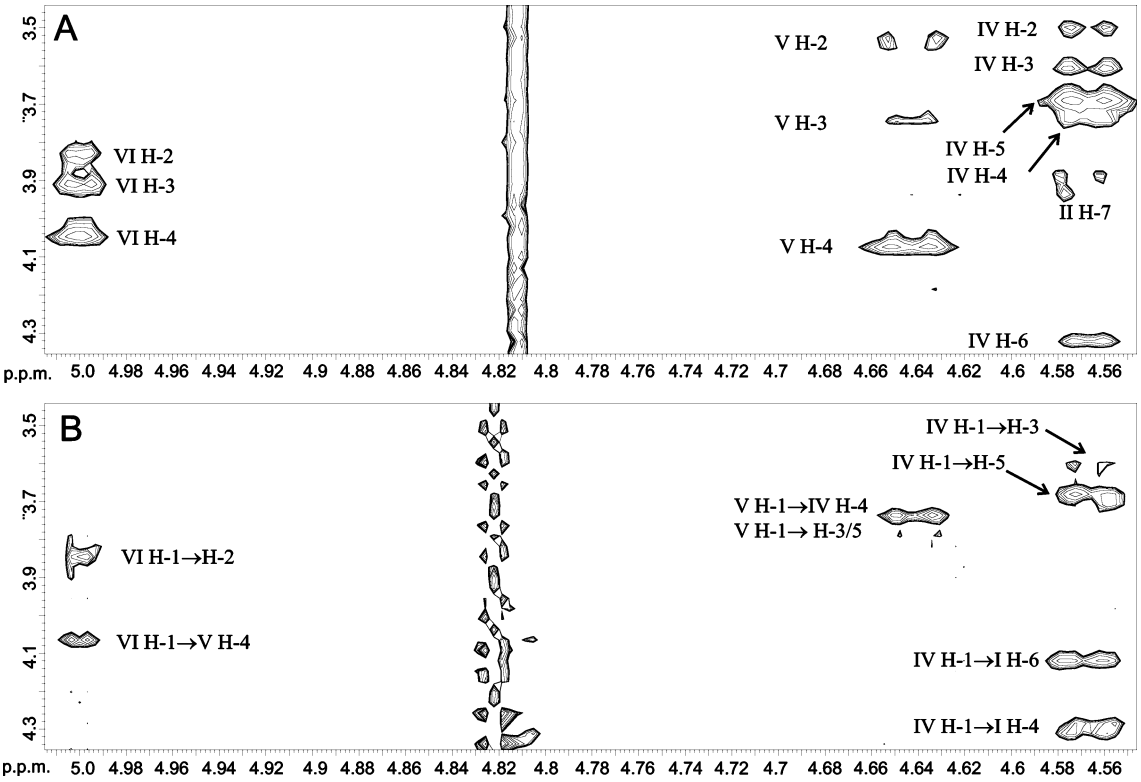

FIGURE 6: (A) Selected region of the two-dimensional gradient and phase sensitive TOCSY spectrum (mixing time of 180 ms) of OS derived from LPS of 1124*lpsA*. Cross-peaks of significant importance are labeled. See Table 6 for an explanation of the Roman numerals. (B) Selected region of the two-dimensional gradient NOESY spectrum (mixing time of 250 ms) of OS derived from LPS of 1124*lpsA*. Cross-peaks of significant importance are labeled.

downfield-shifted H3 and C3 of HepIII. The C3 chemical shift of HepIII was identified in the ^{1}H−^{13}C HMBC spectrum which appeared as a cross-peak between H1 and C3 of HepIII, and the ^{1}H−^{13}C position 3 resonances of HepIII were observed in the ^{1}H−^{13}C HMQC spectrum at δ 4.36/76.9. In addition, the downfield-shifted $H6_{a,b}$ and C6, and a ^{31}P resonance at δ -0.11 coupled to $H6_a$ of residue IV, indicated this residue is substituted with *P*Cho.

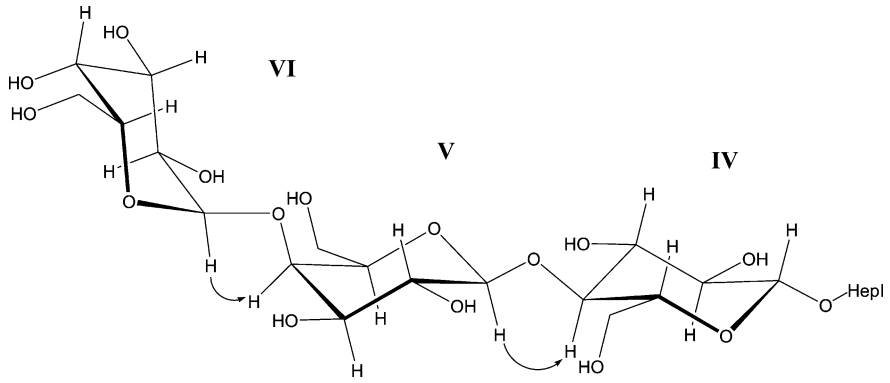

FIGURE 7: Structural representation of the globoside extension of the major Hex3 glycoform in NTHi 1124*lpsA* illustrating the observed transglycosidic NOE connectivities. See Table 6 for an explanation of the Roman numerals.

Scheme 1

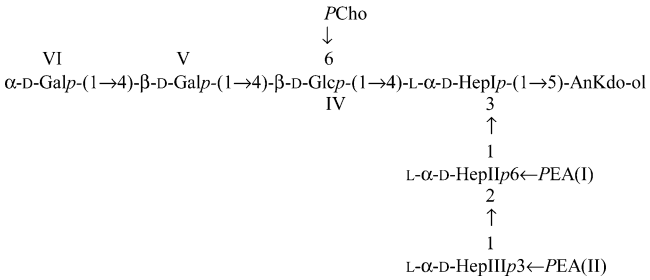

From the combined data for 1124*lpsA*, the structure of the major glycoform in OS1124*lpsA* is proposed as shown in Scheme 1. ESI-MS^n experiments revealed minor glycoforms in OS1124*lpsA* having a HexNAcHexHexHex unit extending from HepI. Since sugar analysis indicated GalN, it is proposed that this residue is linked to VI.

Structure of the Hex4 Glycoform in OS1124lic2A. Sequence analysis of OS1124*lic2A* allowed the identification of glycoforms showing chain elongation from HepI in the same manner as for OS1124*lpsA* and HepIII by a hexose (see above and Table 5). The occurrence of interresidue NOESY connectivities between the various anomeric protons and ring protons in OS1124*lic2A* confirmed an identical structural element as shown in Scheme 1. In addition, in the ^{1}H NMR spectrum of OS1124*lic2A*, an anomeric signal at δ 4.66 could be attributed to a terminal β-D-glucose residue VII. An interresidue NOE between H1 of VII and H1/H2 of HepIII gave evidence for the β-D-Glc*p*-(1→2)-L-α-D-HepIII*p*-(1→ unit. The phosphorylation pattern of *P*EA1, *P*EA2, and *P*Cho in 1124*lic2A* was similar to that in 1124*lpsA*. This was confirmed by the ^{1}H−^{31}P HMQC spectrum which showed the respective phosphorus atoms of *P*EAI, *P*EAII, and *P*Cho at δ 0.53, −0.49, and 0.53 correlated to H6 of HepII at δ 4.57, H3 of HepIII at δ 4.33, and H6$_{a,b}$ at δ 4.22 and 4.37, respectively (see Figure 8). HexNAc-containing glycoforms could not be identified by NMR due to their low abundance, but as for OS1124*lpsA*, sugar analysis together with ESI-MS^n indicated a terminal GalNAc substituting for α-D-Gal*p*. The structure shown in Scheme 2 is proposed for the major Hex4 glycoform in OS1124*lic2A*.

Structure of the Hex4 Glycoform in OS1124lgtC. ESI-MS^n analysis indicated the major Hex4 glycoform of OS1124*lgtC* to carry disaccharide units at both HepI and HepIII of the inner-core triheptosyl unit. NMR analysis of OS1124*lgtC* revealed that HepIII was substituted with a lactose unit [β-D-Gal*p*-(1→4)-β-D-Glc*p*-(1→] as evidenced by interresidue NOESY between proton pairs of VIII H1, VII H4, and HepIII H1 and H2. Furthermore, it was also established that lactose could elongate from HepI as indicated by NOESY data showing cross-peaks between proton pairs V H1, IV H4, and HepI H4 and H6.

In the ^{1}H−^{13}C HMQC spectrum of the 1124*lgtC* mutant, we observed a cross-peak at δ 4.01/41.4 which was not observed in the spectra of the other samples. As glycine is most abundant in the 1124*lgtC* mutant (see Table 2), it was reasonable to assume that this cross-peak corresponded to the methylene nuclei of this residue. This was corroborated by a ^{1}H−^{13}C HMBC spectrum showing ^{1}H−^{13}C cross-peak at δ 4.01/169.0 consistent with coupling between the carbonyl carbon and the CH_2 protons of the glycine residue. The available positions for attachment of the glycine moiety are at O4, O6, and O7, but due to signal overlap, NMR data did not provide information about the exact location of the glycine moiety on the HepIII residue.

No further differences were observed with the isomeric glycoform shown in Scheme 2. Thus, the structure shown in Scheme 3 is proposed for the major Hex4 glycoform in OS1124*lgtC*.

Structure of the Hex6 and Hex7 Glycoforms in OS1124wt. Sequence analysis of OS1124wt revealed the wild-type strain to express a highly heterogeneous mixture of LPS glycoforms having the triheptosyl inner core from which chain elongation only appeared from HepI and HepIII (Table 5). Chain elongations from HepI were the same that appeared in the *lpsA* mutant, and a HexNAc·Hex-Hex-Hex unit appeared to be the most extended oligosaccharide chain from HepIII.

In the ^{1}H NMR spectrum of OS1124wt, anomeric protons of the major Hex6 glycoform corresponding to Gal residues V, VI, VIII, and IX and Glc residues IV and VII were identified at δ 4.86, 4.95, 4.53, 4.97, 4.57, and 4.73, respectively. Interresidue NOEs between VI H1 and V H4, V H1 and IV H4, and IV H1 and HepI H4 and H6 established the sequence of a trisaccharide unit and its attachment point to HepI as α-D-Gal*p*-(1→4)-β-D-Gal*p*-(1→4)-β-D-Glc*p*-(1→4)-L-α-D-Hep*p*-(1→. Interresidue NOEs between IX H1 and VIII H4, VIII H1 and VII H4, and VII H1 and HepIII H1 and H2 established the sequence of a trisaccharide unit and its attachment point to HepIII as α-D-Gal*p*-(1→4)-β-D-Gal*p*-(1→3)-β-D-Glc*p*-(1→2)-L-α-D-Hep*p*-(1→. In summary, the Hex6 glycoform comprised globoside epitopes elongating from HepI and HepIII. In the spectrum, terminal β-D-Gal*p* residues corresponding to V and VIII originating from shorter glycoforms were observed at δ 4.78 and 4.47, respectively.

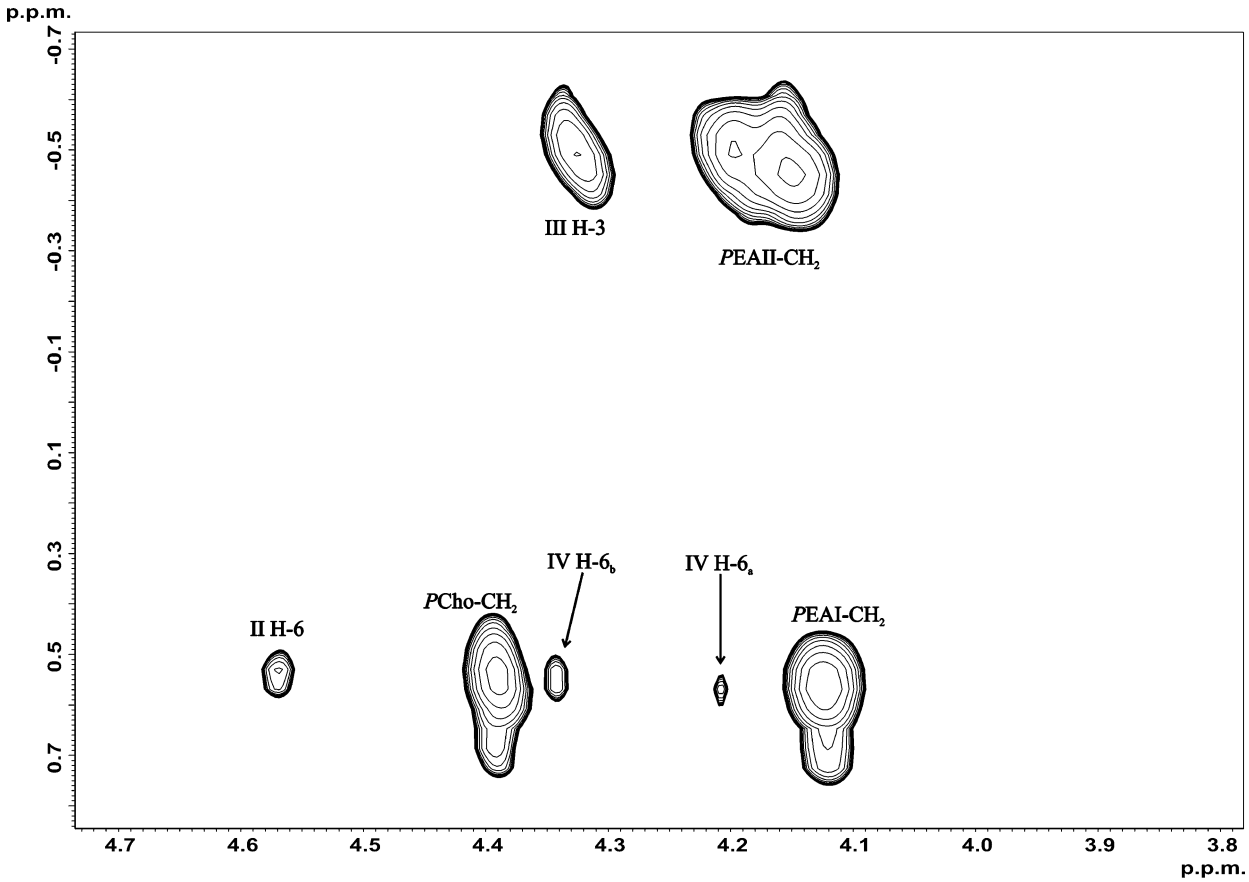

FIGURE 8: Selected region of the two-dimensional $^{1}H-^{31}P$ HMQC spectrum of OS derived from LPS of 1124*lic2A*. Cross-peaks of significant importance are labeled. See Table 6 for an explanation of the Roman numerals.

Scheme 2

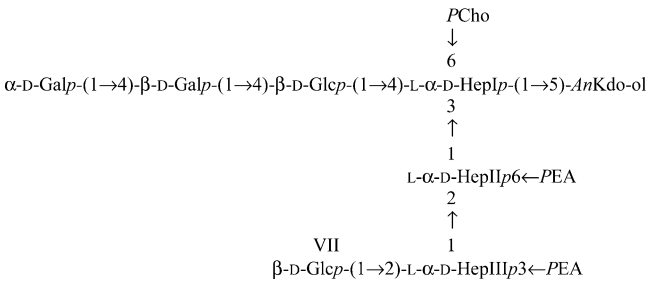

Scheme 3

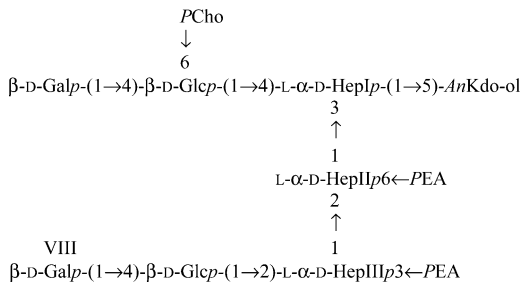

The ^{1}H NMR spectrum also revealed signals at δ 4.68 and 4.94 which could be attributed to terminal α-D-GalNAc residue X and 3-substituted residue IX (α-D-Gal*p*), respectively. An interresidue NOE between H1 of X at δ 4.68 and H3 of the 3-substituted IX at δ 3.98 evidenced the β-D-Gal*p*NAc-(1→3)-α-D-Gal*p*-(1→ element. It was concluded that the Hex7 glycoform in OS1124wt has the structure as shown in Scheme 4.

It is reasonable to assume that the HexNAc·Hex-Hex-Hex elongation from HepI indicated by ESI-MS^{n} also comprises a terminal β-D-Gal*p*NAc-(1→3)-α-D-Gal*p*-(1→.

DISCUSSION

A characteristic feature of *H. influenzae* LPS is the extensive inter- and intrastrain heterogeneity of glycoform structure. This diversity of LPS structure is key to the role of the molecule in both the commensal and disease-causing behavior of the bacterium. NTHi strain 1124 investigated in this study exhibits one of the most heterogeneous LPS structures determined to date. Through a combination of our state-of-the-art structural analyses and use of our extensive knowledge of the genetic blueprint for LPS synthesis, to construct isogenic strains making truncated LPS, we have analyzed the extremely complex glycoforms expressed by this disease-causing isolate and identified some novel patterns.

LPS from NTHi strain 1124 contains the conserved inner-core element L-α-D-Hep*p*-(1→2)-[*P*EA→6]-L-α-D-Hep*p*-(1→3)-[β-D-Glc*p*-(1→4)]-L-α-D-Hep*p*-(1→5)-[*PP*EA→4]-α-Kdo*p*-(2→6)-lipid A of *H. influenzae*. It was found that both the proximal and terminal heptose (HepI and HepIII, respectively) could be substituted by globotetraose chains β-D-Gal*p*NAc-(1→3)-α-D-Gal*p*-(1→4)-β-D-Gal*p*-(1→4)-β-D-Glc*p*-(1→ or the truncated versions thereof (globoside and lactose). Lactose attached to HepI has previously only been observed in NTHi strain 2019 (*4*), and extension by globotetraose and globoside units directly from HepI is a completely new structural variant of *H. influenzae* LPS. Oligosaccharides that mimic the globoside series of mam-

Scheme 4

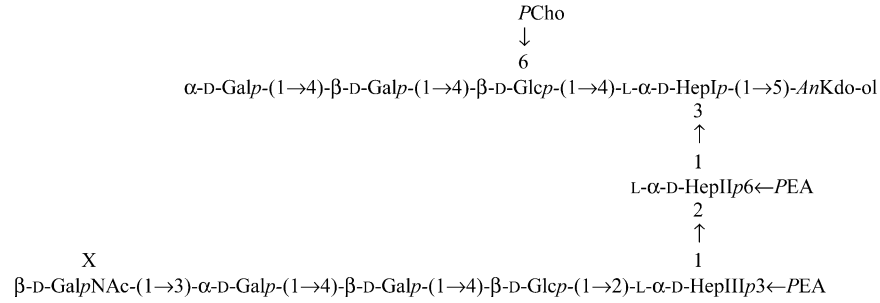

malian glycolipids are common motifs of *H. influenzae* LPS. Globotetraose has been found linked to HepIII in a number of different strains (*9*, *18*, *19*). In addition, globoside oligosaccharides have been found as extensions from a glucose linked to HepI and/or HepII in both capsulate and NTHi (*7*, *20*−*22*). Four genes are involved in the biosynthesis of globotetraose when it is linked to HepIII: *lpsA*, *lic2A*, *lgtC*, and *lgtD* (*26*). In strain Rd, for which the biosynthetic genes were initially identified from the genome sequence, globotetraose is linked to O2 of HepIII, and the four genes are required for sequential addition of the glycoses. *lpsA* is responsible for adding the first glucose residue. *lic2A* is responsible for adding *β*-D-Gal*p* in a 1,4-linkage to the *β*-D-Glc*p* residue. *lgtC* is responsible for adding an α-D-Gal*p* to form globoside [α-D-Gal*p*-(1→4)-*β*-D-Gal*p*-(1→4)-*β*-D-Glc*p*-(1→]. *lgtD* mediates addition of the 1,3-linked terminal *β*-D-Gal*p*NAc. *lpsA*, *lic2A*, *lgtC*, and *lgtD* homologues had been identified in NTHi strain 1124 by PCR-based analysis of LPS biosynthesis genes present in that strain (data not shown)**.** The results presented here show that *lpsA*, *lic2A*, and *lgtC* have identical functions in LPS biosynthesis in NTHi strain 1124 as in strain Rd. In addition, as shown by the structural studies on the *lgtC* mutant strain, *lgtC* is involved in the expression of galabiose as part of the globoside extension from HepI. It has previously been shown that *lgtC* contributes to the expression of terminal galabiose [α-D-Gal*p*-(1→4)-*β*-D-Gal*p*] as part of the globoside epitopes extending from α-D-Glc*p*-(1→4)-HepII and *β*-D-Glc*p*-(1→4)-HepI in type b strains Eagan and RM7004 (*25*). Now, for the first time, we have shown that the *lgtC* gene can be involved in expression of the globoside epitopes from HepI and HepIII in the same strain. Both *lic2A* and *lgtC* are variably expressed, and the mechanism of phase variation is presumed to account for a majority of the LPS structural variation seen in most *H. influenzae* strains. The emphasis placed on making expression of the galabiose highly variable likely reflects its immunodominance and role as a molecular mimic of host structures that can influence survival of *H. influenzae* within different host compartments.

Recently, we have shown that *H. influenzae* can express sialyllacto-*N*-neotetraose [α-Neu5Ac-(2→3)-*β*-D-Gal*p*-(1→4)-*β*-D-Glc*p*NAc-(1→3)-*β*-D-Gal*p*-(1→4)-*β*-D-Glc*p*-(1→] or the related structure (*P*EA→6)-α-D-Gal*p*NAc-(1→6)-*β*-D-Gal*p*-(1→4)-*β*-D-Glc*p*NAc-(1→3)-*β*-D-Gal*p*-(1→4)-*β*-D-Glc*p*-(1→ linked to HepI (*15*). The biosynthesis of the terminal tetrasaccharide moieties was found to resemble that of O-antigen repeat units and is mediated by genes in the *hmg* locus of the *H. influenzae* genome. The tetrasaccharide units are added en bloc, not stepwise, to the glucose linked to HepI [*β*-D-Glc*p*-(1−4)-HepI] (*47*). The gene responsible for initiating synthesis of the tetrasaccharide unit to GlcI is *wbaP*. Therefore, although those structures are extended lactoses, the biosynthesis of the lactose unit from HepI in NTHi strain 1124 is not by this en bloc mechanism and should involve a conventional galactosyltransferase. A possible candidate would be *lic2A*; however, our structural studies on the 1124 *lic2A* mutant showed that the chains extending from HepI were the same as those observed in the wild-type strain. The function of *lic2A* was, as expected, in the expression of lactose from HepIII. No further homologues of *lic2A* were identified in strain 1124 following PCR and Southern analyses of DNA isolated from the wild-type and mutant strains (data not shown). The phase variable *lex2* locus has been shown to encode a glucosyltransferase important in further oligosaccharide extension from *β*-D-Glc*p*-(1−4)-HepI (*31*). Interestingly, NTHi strain 1124 also possesses the *lex2* gene, but no clear evidence for the *β*-D-Glc*p*-(1→4)-*β*-D-Glc*p*-(1→ epitope could be found in either the wild-type or mutant strains. We could, however, by the use of ESI-MS^n identify traces of glycoforms having Hex4 extensions from HepI. A galabiose-containing tetrasaccharide extension from HepI is found in type b strains with the structure α-Gal*p*-(1→4)-*β*-D-Gal*p*-(1→4)-*β*-D-Glc*p*-(1→4)-*β*-D-Glc*p*-(1→ (*22*). One could speculate that this is an alternative structure extending from HepI in NTHi 1124 when *lex2* is active. It is possible that lex2 and the still unidentified galactosyltransferase are competing and the galactosyltransferase is dominant, the phase variable *lex2* is predominantly not expressed under our in vitro culture conditions, or lex2 in this strain of NTHi has galactosyltransferase activity. We are currently investigating these possibilities.

A majority of typeable and nontypeable strains of *H. influenzae* have the potential to incorporate Neu5Ac into their LPS (*33*, *44*), and strains expressing this sugar are more resistant to the bactericidal activity of normal human serum in vitro. Incorporation of Neu5Ac in *H. influenzae* LPS depends on an exogenous source of the sugar. Recently, we have shown that host-derived Neu5Ac is incorporated in *H. influenzae* LPS and is a major virulence factor in experimental otitis media (*35*). Three genes have been described as encoding sialyltransferases in *H. influenzae*, *lic3A*, *lsgB*, and *siaA*. *lic3A* encodes the phase variable α-2,3-sialyltransferase sialylating terminal lactose extending from HepIII, and *lsgB* and *siaA* are involved in sialylation of the lacto-*N*-neotetraose units, described above, extending from HepI (*34*, *48*). The level of sialylation in *H. influenzae* LPS is generally low, and detailed structural analysis of sialylated glycoforms has only been possible for less heterogeneous strains grown under appropriate conditions to maximize sialylated glycoform expression (*13*, *17*).

Analysis has shown that NTHi strain 1124 contains each of the sialyltransferase genes, *lic3A*, *lsgB*, and *siaA*. Initially, sialylation of this strain was demonstrated by us in a survey made on 24 NTHi strains using HPAEC-PAD in combination with neuraminidase treatment (*44*). A more detailed characterization of the sialylated glycoforms in NTHi strain 1124 could be done here by using precursor ion scan CE-MS/MS (Table 5 and Figure 1). We found that 1124wt expresses sialylated glycoforms ranging from Hex2 to Hex5 species. Most predominant was the glycoform with the Neu5Ac·*P*Cho·Hex_4·Hep_3·*P*EA_3·*P*·Kdo·lipid A-OH composition. In the *lgtC* mutant, a disialylated Hex4 glycoform with the $Neu5Ac_2$·*P*Cho·Hex_4·Hep_3·*P*EA_3·*P*·Kdo·lipid A-OH composition predominated, which is consistent with the observation made for strain Rd whereby LgtC competes with Lic3A for the same acceptor and the Rd*lgtC* mutant expressed high levels of sialyllactose from HepIII (*34*). The nature of a disialylated species in 1124 *lgtC* and also 1124wt could involve either monosialylation at two different sites or disialylation at one site. Disialylated (Neu5Ac−Neu5Ac) extensions from HepIII have been observed previously (*16*, *33*). Evidence for sialylated epitopes extending from HepI was obtained by analysis of the *lpsA* mutant which showed both mono- and disialylated Hex2 glycoforms. This provides compelling evidence for expression of mono- and disialylated structures extending from HepI in the parent strain. It is tempting to assume that *lic3A* is involved in the biosynthesis of this epitope. We are currently investigating the genetic basis of LPS sialylation in NTHi 1124 and the role of the sialylated glycoforms in the biology of the bacterium.

Chain extension from HepII was not detected in NTHi 1124, and thus, one key aspect of LPS heterogeneity is not evident in this isolate. This is consistent with the PCR-based analysis of LPS biosynthesis genes which indicated that the gene responsible for initiating chain elongation from HepII, *lic2C*, is absent in this strain.

In addition to the stereochemistry, the substitution pattern and sequence of the sugar residues attached to the common triheptosyl unit, the location, the type, and the frequency of noncarbohydrate substituents can have a profound affect on LPS structure and biological function.

It has been established that a contributing factor to colonization and virulence of *H. influenzae* is the presence of *P*Cho in LPS (*49*). Analysis of 1124wt showed that *lic1*, the phase variable locus regulating the expression of *P*Cho, was present in this strain, a result consistent with the structural analysis in this study.

In several *H. influenzae* strains, the core region has been found (*4*, *7*, *20*, *25*) to be substituted by a phosphate or a *P*EA group in addition to the conserved 6-substituted *P*EA group at HepII and the pyrophosphoethanolamine (*PP*EA) group at the Kdo residue. However, in most of those strains, additional phosphorylation was incomplete and/or very minor, making elucidation of fine structural details impossible. Recently, however, in NTHi 981, a strain having complete substitution with *P*EA at HepIII, we could show that this group substituted at the O3 position (*20*). NTHi 1124 is another strain in which HepIII is highly substituted with *P*EA, and its position could be located at O3 as well. The gene involved in expression of *P*EA at O6 of HepII has been recently identified as *lpt6* (*50*). The gene adding *P*EA to O3 of HepIII is still unknown and is currently under investigation.

Ester-linked glycine has been shown to be a prominent substituent in the core region of *H. influenzae* LPS. All strains investigated so far express minor amounts of this amino acid (*45*). The most common site for this substituent is HepIII, but it can also been found at HepII or Kdo. In strain 1124, the position of glycine is indicated at HepIII. The biological significance of glycine with respect to the role of LPS of *H. influenzae* is not clear. *O*-Acetyl groups which are found in approximately 50% of all strains investigated by us are absent in NTHi 1124.

In conclusion, these analyses have shown that the synergy between genetic and structural analyses is tremendously powerful in the investigation of *H. influenzae* LPS. Structural analysis has been a key in determining the genetic blueprint for LPS synthesis in *H. influenzae*; however, genetic manipulation of key genes has been a powerful tool in aiding the structural analysis, and this is still an ongoing process as novel structures and genes are found.

ACKNOWLEDGMENT

We thank the members of the Finnish Otitis Media Study group at the National Health Institute in Finland for the provision of NTHi strains from the nasopharynx, obtained as part of the Finnish Otitis Media Cohort study. Gaynor Randle is acknowledged for help with constructing mutant strains and for the culture of bacteria. Kathy Makepeace is acknowledged for help with electrophoretic analysis of LPS samples.

REFERENCES

1. Campagnari, A. A., Gupta, M. R., Dudas, K. C., Murphy, T. F., and Apicella, M. A. (1987) Antigenic diversity of lipooligosaccharides of nontypable *Haemophilus influenzae*, *Infect. Immun. 55*, 882−887.
2. Moxon, E. R. (1985) The molecular basis of *Haemophilus influenzae* virulence, *J. R. Coll. Physicians London 19*, 174−178.
3. Kimura, A., and Hansen, E. J. (1986) Antigenic and phenotypic variations of *Haemophilus influenzae* type b lipopolysaccharide and their relationship to virulence, *Infect. Immun. 51*, 69−79.
4. Phillips, N. J., Apicella, M. A., Griffiss, J. M., and Gibson, B. W. (1992) Structural characterization of the cell surface lipooligosaccharides from a nontypable strain of *Haemophilus influenzae*, *Biochemistry 31*, 4515−4526.
5. Schweda, E. K., Hegedus, O. E., Borrelli, S., Lindberg, A. A., Weiser, J. N., Maskell, D. J., and Moxon, E. R. (1993) Structural studies of the saccharide part of the cell envelope lipopolysaccharide from *Haemophilus influenzae* strain AH1−3 (lic3+), *Carbohydr. Res. 246*, 319−330.
6. Schweda, E. K., Jansson, P. E., Moxon, E. R., and Lindberg, A. A. (1995) Structural studies of the saccharide part of the cell envelope lipooligosaccharide from *Haemophilus influenzae* strain galEgalK, *Carbohydr. Res. 272*, 213−224.
7. Masoud, H., Moxon, E. R., Martin, A., Krajcarski, D., and Richards, J. C. (1997) Structure of the variable and conserved lipopolysaccharide oligosaccharide epitopes expressed by *Haemophilus influenzae* serotype b strain Eagan, *Biochemistry 36*, 2091−2103.
8. Risberg, A., Schweda, E. K., and Jansson, P. E. (1997) Structural studies of the cell-envelope oligosaccharide from the lipopolysaccharide of *Haemophilus influenzae* strain RM.118−28, *Eur. J. Biochem. 243*, 701−707.
9. Risberg, A., Masoud, H., Martin, A., Richards, J. C., Moxon, E. R., and Schweda, E. K. (1999) Structural analysis of the lipopolysaccharide oligosaccharide epitopes expressed by a capsule-deficient strain of *Haemophilus influenzae* Rd, *Eur. J. Biochem. 261*, 171−180.

10. Risberg, A., Alvelius, G., and Schweda, E. K. (1999) Structural analysis of the lipopolysaccharide oligosaccharide epitopes expressed by *Haemophilus influenzae* strain RM.118−26, *Eur. J. Biochem. 265*, 1067−1074.
11. Rahman, M. M., Gu, X. X., Tsai, C. M., Kolli, V. S., and Carlson, R. W. (1999) The structural heterogeneity of the lipooligosaccharide (LOS) expressed by pathogenic non-typeable *Haemophilus influenzae* strain NTHi 9274, *Glycobiology 9*, 1371−1380.
12. Schweda, E. K., Brisson, J. R., Alvelius, G., Martin, A., Weiser, J. N., Hood, D. W., Moxon, E. R., and Richards, J. C. (2000) Characterization of the phosphocholine-substituted oligosaccharide in lipopolysaccharides of type b *Haemophilus influenzae*, *Eur. J. Biochem. 267*, 3902−3913.
13. Månsson, M., Bauer, S. H., Hood, D. W., Richards, J. C., Moxon, E. R., and Schweda, E. K. (2001) A new structural type for *Haemophilus influenzae* lipopolysaccharide. Structural analysis of the lipopolysaccharide from nontypeable *Haemophilus influenzae* strain 486, *Eur. J. Biochem. 268*, 2148−2159.
14. Cox, A. D., Masoud, H., Thibault, P., Brisson, J. R., van der Zwan, M., Perry, M. B., and Richards, J. C. (2001) Structural analysis of the lipopolysaccharide from the nontypable *Haemophilus influenzae* strain SB 33, *Eur. J. Biochem. 268*, 5278−5286.
15. Cox, A. D., Hood, D. W., Martin, A., Makepeace, K. M., Deadman, M. E., Li, J., Brisson, J. R., Moxon, E. R., and Richards, J. C. (2002) Identification and structural characterization of a sialylated lacto-N-neotetraose structure in the lipopolysaccharide of *Haemophilus influenzae*, *Eur. J. Biochem. 269*, 4009−4019.
16. Schweda, E. K., Li, J., Moxon, E. R., and Richards, J. C. (2002) Structural analysis of lipopolysaccharide oligosaccharide epitopes expressed by non-typeable *Haemophilus influenzae* strain 176, *Carbohydr. Res. 337*, 409−420.
17. Månsson, M., Hood, D. W., Li, J., Richards, J. C., Moxon, E. R., and Schweda, E. K. (2002) Structural analysis of the lipopolysaccharide from nontypeable *Haemophilus influenzae* strain 1003, *Eur. J. Biochem. 269*, 808−818.
18. Schweda, E. K., Landerholm, M. K., Li, J., Richard Moxon, E., and Richards, J. C. (2003) Structural profiling of lipopolysaccharide glycoforms expressed by non-typeable *Haemophilus influenzae*: Phenotypic similarities between NTHi strain 162 and the genome strain Rd, *Carbohydr. Res. 338*, 2731−2744.
19. Månsson, M., Hood, D. W., Moxon, E. R., and Schweda, E. K. (2003) Structural diversity in lipopolysaccharide expression in nontypeable *Haemophilus influenzae*. Identification of L-glycerol-D-manno-heptose in the outer-core region in three clinical isolates, *Eur. J. Biochem. 270*, 610−624.
20. Månsson, M., Hood, D. W., Moxon, E. R., and Schweda, E. K. (2003) Structural characterization of a novel branching pattern in the lipopolysaccharide from nontypeable *Haemophilus influenzae*, *Eur. J. Biochem. 270*, 2979−2991.
21. Yildirim, H. H., Hood, D. W., Moxon, E. R., and Schweda, E. K. (2003) Structural analysis of lipopolysaccharides from *Haemophilus influenzae* serotype f. Structural diversity observed in three strains, *Eur. J. Biochem. 270*, 3153−3167.
22. Masoud, H., Martin, A., Thibault, P., Moxon, E. R., and Richards, J. C. (2003) Structure of extended lipopolysaccharide glycoforms containing two globotriose units in *Haemophilus influenzae* serotype b strain RM7004, *Biochemistry 42*, 4463−4475.
23. Landerholm, M. K., Li, J., Richards, J. C., Hood, D. W., Moxon, E. R., and Schweda, E. K. (2004) Characterization of novel structural features in the lipopolysaccharide of nondisease associated nontypeable *Haemophilus influenzae*, *Eur. J. Biochem. 271*, 941−953.
24. Weiser, J. N., Williams, A., and Moxon, E. R. (1990) Phase-variable lipopolysaccharide structures enhance the invasive capacity of *Haemophilus influenzae*, *Infect. Immun. 58*, 3455−3457.
25. Hood, D. W., Deadman, M. E., Allen, T., Masoud, H., Martin, A., Brisson, J. R., Fleischmann, R., Venter, J. C., Richards, J. C., and Moxon, E. R. (1996) Use of the complete genome sequence information of *Haemophilus influenzae* strain Rd to investigate lipopolysaccharide biosynthesis, *Mol. Microbiol. 22*, 951−965.
26. Hood, D. W., Cox, A. D., Wakarchuk, W. W., Schur, M., Schweda, E. K., Walsh, S. L., Deadman, M. E., Martin, A., Moxon, E. R., and Richards, J. C. (2001) Genetic basis for expression of the major globotetraose-containing lipopolysaccharide from *H. influenzae* strain Rd (RM118), *Glycobiology 11*, 957−967.
27. Hood, D. W., Deadman, M. E., Cox, A. D., Makepeace, K., Martin, A., Richards, J. C., and Moxon, E. R. (2004) Three genes, lgtF, lic2C and lpsA, have a primary role in determining the pattern of oligosaccharide extension from the inner core of *Haemophilus influenzae* LPS, *Microbiology 150*, 2089−2097.
28. Weiser, J. N., Maskell, D. J., Butler, P. D., Lindberg, A. A., and Moxon, E. R. (1990) Characterization of repetitive sequences controlling phase variation of *Haemophilus influenzae* lipopolysaccharide, *J. Bacteriol. 172*, 3304−3309.
29. Jarosik, G. P., and Hansen, E. J. (1994) Identification of a new locus involved in expression of *Haemophilus influenzae* type b lipooligosaccharide, *Infect. Immun. 62*, 4861−4867.
30. Hood, D. W., Deadman, M. E., Jennings, M. P., Bisercic, M., Fleischmann, R. D., Venter, J. C., and Moxon, E. R. (1996) DNA repeats identify novel virulence genes in *Haemophilus influenzae*, *Proc. Natl. Acad. Sci. U.S.A. 93*, 11121−11125.
31. Griffin, R., Cox, A. D., Makepeace, K., Richards, J. C., Moxon, E. R., and Hood, D. W. (2003) The role of lex2 in lipopolysaccharide biosynthesis in *Haemophilus influenzae* strains RM7004 and RM153, *Microbiology 149*, 3165−3175.
32. Weiser, J. N., Shchepetov, M., and Chong, S. T. (1997) Decoration of lipopolysaccharide with phosphorylcholine: A phase-variable characteristic of *Haemophilus influenzae*, *Infect. Immun. 65*, 943−950.
33. Hood, D. W., Makepeace, K., Deadman, M. E., Rest, R. F., Thibault, P., Martin, A., Richards, J. C., and Moxon, E. R. (1999) Sialic acid in the lipopolysaccharide of *Haemophilus influenzae*: Strain distribution, influence on serum resistance and structural characterization, *Mol. Microbiol. 33*, 679−692.
34. Hood, D. W., Cox, A. D., Gilbert, M., Makepeace, K., Walsh, S., Deadman, M. E., Cody, A., Martin, A., Mansson, M., Schweda, E. K., Brisson, J. R., Richards, J. C., Moxon, E. R., and Wakarchuk, W. W. (2001) Identification of a lipopolysaccharide α-2,3-sialyltransferase from *Haemophilus influenzae*, *Mol. Microbiol. 39*, 341−350.
35. Bouchet, V., Hood, D. W., Li, J., Brisson, J. R., Randle, G. A., Martin, A., Li, Z., Goldstein, R., Schweda, E. K., Pelton, S. I., Richards, J. C., and Moxon, E. R. (2003) Host-derived sialic acid is incorporated into *Haemophilus influenzae* lipopolysaccharide and is a major virulence factor in experimental otitis media, *Proc. Natl. Acad. Sci. U.S.A. 100*, 8898−8903.
36. Cody, A. J., Field, D., Feil, E. J., Stringer, S., Deadman, M. E., Tsolaki, A. G., Gratz, B., Bouchet, V., Goldstein, R., Hood, D. W., and Moxon, E. R. (2003) High rates of recombination in otitis media isolates of non-typeable *Haemophilus influenzae*, *Infect. Genet. Evol. 3*, 57−66.
37. Herriott, R. M., Meyer, E. M., and Vogt, M. (1970) Defined nongrowth media for stage II development of competence in *Haemophilus influenzae*, *J. Bacteriol. 101*, 517−524.
38. Galanos, C., Lüderitz, O., and Westphal, O. (1969) A new method for the extraction of R lipopolysaccharides, *Eur. J. Biochem. 9*, 245−249.
39. Holst, O., Brade, L., Kosma, P., and Brade, H. (1991) Structure, serological specificity, and synthesis of artificial glycoconjugates representing the genus-specific lipopolysaccharide epitope of *Chlamydia* spp., *J. Bacteriol. 173*, 1862−1866.
40. Sawardeker, J. S., Sloneker, J. H., and Jeanes, A. (1965) Quantitative determination of monosaccharides as their alditol acetates by gas liquid chromatography, *Anal. Chem. 37*, 1602−1604.
41. Gerwig, G. J., Kamerling, J. P., and Vliegenhart, J. F. G. (1979) Determination of the absolute configuration of monosaccharides in complex carbohydrates by capillary GLC, *Carbohydr. Res. 77*, 1−7.
42. Blakeney, A. B., and Stone, B. A. (1985) Methylation of carbohydrates with lithium methylsulphinyl carbanion, *Carbohydr. Res. 140*, 319−324.
43. Helander, I. M., Lindner, B., Brade, H., Altmann, K., Lindberg, A. A., Rietschel, E. T., and Zähringer, U. (1988) Chemical structure of the lipopolysaccharide of *Haemophilus influenzae* strain I-69 Rd-/b+. Description of a novel deep-rough chemotype, *Eur. J. Biochem. 177*, 483−492.
44. Bauer, S. H., Månsson, M., Hood, D. W., Richards, J. C., Moxon, E. R., and Schweda, E. K. (2001) A rapid and sensitive procedure for determination of 5-*N*-acetyl neuraminic acid in lipopolysaccharides of *Haemophilus influenzae*: A survey of 24 non-typeable *H. influenzae* strains, *Carbohydr. Res. 335*, 251−260.
45. Li, J., Bauer, S. H. J., Månsson, M., Moxon, E. R., Richards, J. C., and Schweda, E. K. H. (2001) Glycine is a common substituent of the inner-core in *Haemophilus influenzae* lipopolysaccharide, *Glycobiology 11*, 1009−1015.

46. Kussak, A., and Weintraub, A. (2002) Quadrupole ion-trap mass spectrometry to locate fatty acids on lipid A from Gram-negative bacteria, *Anal. Biochem. 307*, 131−137.
47. Hood, D. W., Randle, G., Cox, A. D., Makepeace, K., Li, J., Schweda, E. K., Richards, J. C., and Moxon, E. R. (2004) Biosynthesis of cryptic lipopolysaccharide glycoforms in *Haemophilus influenzae* involves a mechanism similar to that required for O-antigen synthesis, *J. Bacteriol. 186*, 7429−7439.
48. Jones, P. A., Samuels, N. M., Phillips, N. J., Munson, R. S., Jr., Bozue, J. A., Arseneau, J. A., Nichols, W. A., Zaleski, A., Gibson, B. W., and Apicella, M. A. (2002) *Haemophilus influenzae* type b strain A2 has multiple sialyltransferases involved in lipooligosaccharide sialylation, *J. Biol. Chem. 277*, 14598−14611.
49. Weiser, J. N., Pan, N., McGowan, K. L., Musher, D., Martin, A., and Richards, J. (1998) Phosphorylcholine on the lipopolysaccharide of *Haemophilus influenzae* contributes to persistence in the respiratory tract and sensitivity to serum killing mediated by C-reactive protein, *J. Exp. Med. 187*, 631−640.
50. Wright, J. C., Hood, D. W., Randle, G. A., Makepeace, K., Cox, A. D., Li, J., Chalmers, R., Richards, J. C., and Moxon, E. R. (2004) lpt6, a gene required for addition of phosphoethanolamine to inner-core lipopolysaccharide of *Neisseria meningitidis* and *Haemophilus influenzae*, *J. Bacteriol. 186*, 6970−6982.

BI047480H